MECHANISMS OF SOFT PALATE CLOSURE IN HUMAN EMBRYOS

by

Melanie Mattson

B.Sc.Hons, The University of Calgary, 2005

DDS, The University of Alberta, 2009

A THESIS SUBMITTED IN PARTIAL FULFILLMENT OF

THE REQUIREMENTS FOR THE DEGREE OF

MASTER OF SCIENCE

in

THE FACULTY OF GRADUATE AND POSTDOCTORAL STUDIES

THE UNIVERSITY OF BRITISH COLUMBIA

(Vancouver)

August 2013

Abstract

Objectives: The human secondary palate forms between 6-12 weeks of gestation. There has been controversy as to whether palatal shelves in the soft palate join by fusion similar to the hard palate, or whether merging and proliferation of the mesenchyme at the posterior edge of the developing hard palate is the mechanism. The purpose of this study is to examine the mode of soft palate closure in a more representative sample than was used in the single previous study on which all textbooks are based.

Methods: Serial sections of secondary palates from 13 human fetuses from 54-74-days of development post conception were stained, photographed and imported into WinSurf 3D software. Anatomical structures were traced including the palatal shelves, midline epithelial seam and palatine aponeurosis, the images aligned and then stacked to create a 3D representation.

Results: We analyzed the following numbers of specimens: 54-days-2; 57-days-4; 59 days -2; 64-days-1; 67-days-1; 70-days–2; 74-days-1. At 54-days, a midline seam is present close to the hard palate but more posteriorly the soft palate is open. Between 57 and 59 days a thick midline seam is observed throughout the soft palate. There is some variability between specimens such that the soft palate was closed early in one 59 day specimen and open in a 67-day specimen. One 70-day specimen had no seam whereas the other retained the seam. By 74-days the specimen had complete soft palate union with the presence of a continuous palatine aponeurosis. Overall, our sample included a total of 7 fetuses with a midline seam in the soft palate.

Conclusions: The formation of a bilayered epithelial seam followed by breakdown of the seam and mesenchymal fusion is the primary mode of soft palate formation in humans. Epithelial seam removal is rapid and could explain why a seam was not observed in earlier studies.

Preface

Human conceptuses were obtained from the University of Washington between 1988 and 1991 by Dr. V. M. Diewert.

The work was carried out under UBC Human Ethics approval # H08-02576. This protocol was approved Nov. 18, 2011 and is renewed annually.

Work was supported by Faculty of Dentistry research funds to JMR.

Table of Contents

List of Tables

List of Figures

List of Abbreviations

BMP: bone morphogenetic protein

BSA: bovine serum albumin

CL/P: cleft lip and palate

CPO: cleft palate only

DAB: detection and visualization of antibody binding

ddH_2O: double distilled water

EDTA: Ethylenediaminetetraacetic acid

EtOH: ethanol

H&E: hematoxalin and eosin

IgG: Immunoglobulin G

lvp: levator veli palatini

mee: medial edge epithelium

mes: midline epithelial seam

PBS: phosphate buffered saline

PCNA: proliferating cell nuclear antigen

PFA: paraformaldehyde

SHH: Sonic Hedgehog

tvp: tensor veli palatini

TUNEL: terminal deoxynucleotidyl transferase nick-end labeling

VPI: velopharyngeal insufficiency

Acknowledgements

I would like to offer my sincerest thanks to Dr. Joy Richman for all her help and support over the past three years. Without her I would not have been able to complete this project.

Many thanks to Dr. Virginia Diewert, Kathy Fu, and the members of the Richman lab who have helped me along the way.

Special thanks are owed to my parents, whose have supported me throughout my years of education, both morally and financially.

CHAPTER 1 - INTRODUCTION

Staging of human embryos

In order to compare my results to those of others, it is first important to review the challenges with staging human embryos. As we shall see, when microscopic anatomy is being analyzed there are considerable variations in development for a given chronological age. Therefore accurate staging is essential to compare my results to studies of others.

There are many different ways by which a human embryo or fetus can be staged. It is of utmost importance that the age of conception be determined as accurately as possible for research purposes, as huge developmental changes can be seen in an embryo or fetus over the course of a few hours to a few days. A general estimate can be determined by the menstrual age, which is calculated based on the last reported menstruation. Menstrual age is a value commonly used by obstetricians. Assuming ovulation and fertilization occurred 14 days after the first day of the last menstruation, fertilization age is calculated as 14 days younger than the menstrual age (Sperber and Guttman, 2010) . These dates are open to interpretation and rely on patients to correctly report the first day of their last menstrual cycle. To improve the accuracy of dating a human conceptus, other measurements may be utilized. Crown-rump length is the earliest measurement that can accurately be used to date a developing embryo. Crown-rump length can reliably be used on an embryo as young as 6 weeks. Crown-rump length involves measuring the height of the fetus when it is in a passive C-shape, not stretched out, from the tip of the head to the base

of the buttocks. When this method is being used on a live fetus via ultrasound, a best of three measurements should be taken. Maternal factors can alter the accuracy of the crown-rump length, as maternal age, smoking and folic acid intake all play a role in the size of the fetus (Altman and Chitty, 1997) . In fetuses aged 13-25 weeks, femur length can also be used to estimate gestational age (Altman and Chitty, 1997).

Two methods based on the size of the cranium exist for dating human fetuses, these are head circumference and the biparietal diameter. Head circumference is a measurement independent of head shape, whereas the biparietal diameter is dependent on head shape, and requires the cephalic index to be used to account for a dolicocephalic versus brachycephalic head type. It has been recommended that due to the inaccuracy of the results, that the biparietal diameter be replaced with head circumference measurements (Altman and Chitty, 1997; Hadlock et al., 1981). Head circumference is calculated by taking an anteroposterior and a biparietal measurement through a horizontal section of a fetal head at the level of the ventricles. Mathematical formulas are utilized to calculate the head circumference value, then this value is used in an additional formula to determine the gestational age (Altman and Chitty, 1997).

Streeter was one of the first individuals to attempt to quantify gestational age of embryos in the early 1900's, based on measured values such as weight, head size and foot length (Streeter, 1920) . These collections he viewed would ultimately become part of the Carnegie Collection, an atlas by which embryologic development is based (O'Rahilly and Muller, 2010). Another investigator (Hern, 1984) analyzed 1800 tissue specimens ranging from 10-24 weeks obtained post-abortion and measured weight, knee to heel length, biparietal diameter, placental weight and

amniotic fluid volume. He preferred foot length as a guide, as this value is easily obtainable and is not subject to significant operator error. Most recently, O'Rahilly and Muller re-evaluated the staging of the Carnegie collection (O'Rahilly and Muller, 2010). They commented that crown-rump lengths should be used with caution, as this is difficult values to obtain due to arbitrary landmarks, and instead, the greatest length of the specimen (excluding the lower limbs) should be used. In general female embryos and fetuses will be smaller and shorter in length than male embryos. The specimens in my study have had their ages determined by a combination of last reported menstrual period, crown-rump length and foot size.

1.1. Development of the primary palate

Primary palate or lip formation begins during the 4th week of human development. The neural crest cells begin to migrate away from the neural tube into the region of the developing face at 21 days gestation (O'Rahilly and Muller, 2007; Sperber and Guttman, 2010). Shortly after, by 24 days, the frontonasal process, and the maxillary and mandibular processes from the first arch have formed and have surrounded the primitive stomodeum (Mossey et al., 2009; Sperber and Guttman, 2010). Initially there is a buccopharyngeal membrane separating the oral cavity from the developing gastrointestinal tract. The epithelial lining of all of the structures anterior to the membrane is of ectodermal origin, and the lining of everything posterior to the membrane is thought to be of endodermal origin. The position of the precise line dividing ectodermal and endodermal epithelium in the

oral cavity is not known. As early as 28 days the buccopharyngeal membrane ruptures, connecting the two cavities (Sadler and Langman, 2010a; Sperber and Guttman, 2010). The next major feature of the face to form is the nose. Initially nasal placodes form as ectodermal thickenings on the frontonasal process and by 33 days the placodes have invaginated into the underlying mesenchyme to become nasal pits. The medial nasal prominences are medial to the nasal pits while the lateral nasal prominences are lateral (Sadler and Langman, 2010a; Sperber and Guttman, 2010). On each side of the stomodeum, the maxillary prominences bud outwards. The inferior mandibular prominences complete the circle of facial prominences that ring the stomodeum. The fate of each prominence is distinct. The medial nasal prominences contribute to the facial midline, nasal septum, centre of the nose, philtrum, premaxilla and 4 incisors. The lateral nasal prominences contribute to the nasal turbinates as shown in chicken experiments (MacDonald et al., 2004). The maxillary prominences form the bones of the palate and upper jaw (Lee et al., 2004) as well as all teeth posterior to the lateral incisors. The mandibular prominences form the entire mandible, parts of the temporomandibular joint as well as ossicles in the inner ear.

As these facial prominences mature, there are two developmental processes bringing the facial prominences together, merging and fusion. Merging involves removal of a groove or furrow between partially attached developmental structures by the migration and proliferation of underlying mesenchymal cells to fill in these grooves (Sperber and Guttman, 2010). Fusion, on the other hand, occurs when two epithelial-lined structures contact and create a bilayered epithelial seam, which is

thought to be removed by apoptosis, epithelial to mesenchymal cell transformation, and cell migration to adjacent epithelia. Most of the work on fusion in the face was carried out on the secondary palate (Fitchett and Hay, 1989; Shuler, 1995; Sperber and Guttman, 2010) so it is not clear whether all of the aforementioned mechanisms are at play during primary palate formation. The only data on EMT in the primary palate comes from the chicken embryo in which the seam between the frontonasal mass and maxillary prominence was seen to transform to mesenchyme (Sun et al., 2000). In the mouse model, there is typically apoptosis at the point of contact of the medial nasal and maxillary prominences (Jiang et al., 2006). Fusion in the primary palate occurs in 41 day embryos when the maxillary prominences contact the medial and lateral nasal processes (Sadler and Langman, 2010a; Sperber and Guttman, 2010). The point of contact between the maxillary, medial and lateral nasal prominences is the area most susceptible to clefting. Merging takes place in the paired medial nasal processes, and a result of this process, the intermaxillary segment is formed. Two other places in the face undergo merging, The lower jaw also develops by merging of the midline of the mandibular prominences in a posterior to anterior fashion (Oostrom et al., 1996). Finally, the maxillary and lateral nasal processes are separated by a deep furrow that fills in by merging. Failure of merging in this region leads to an exposed nasolacrimal duct . Thus by the end of 47 days, the primary palate has completed development and residual grooves are being filled in by merging.

1.2. Secondary palate development

1.3.1 Embryonic period

During the 6th week of gestation, the secondary palate begins to develop (Dixon et al., 2011). It starts initially as two outgrowths from the maxillary prominences which are oriented in a vertical direction and lay on either side of the tongue (Greene and Pisano, 2010; Sadler and Langman, 2010a). During the 8th week of development, the palatal shelves reorient in to a horizontal position over in just a few hours (Bush and Jiang, 2012; Gritli-Linde, 2007; Sadler and Langman, 2010a; Sperber and Guttman, 2010). While reorientation is occurring, the mandible is elongating and the fetal head tilts upwards. Both of these events help move the tongue out from between the shelves (Diewert, 1985; Diewert, 1986). The palatal shelves continue to grow towards each other and contact at the medial edge epithelia. A transient bilayered epithelium or midline epithelial seam (mes) is formed at this time (Gritli-Linde, 2007; Mossey et al., 2009). This process of fusion requires adherence of the two epithelia, which occurs via cell adhesion molecules and desmosomes (Mogass et al., 2000; Mossey et al., 2009). Growth factors are also important in palatal fusion as well. Transforming growth factor α (TGFα), epidermal growth factor receptor (EGFR) and members of the transforming growth factor β superfamily (TGFβ) have all been shown to play a role in fusion of the palatal shelves (Cui et al., 2003; Cui et al., 2005; Dudas et al., 2004; Kaartinen et al., 1997; Kaartinen et al., 1995; Miettinen et al., 1999; Proetzel et al., 1995). After the palatal

shelves have contacted and fused, the midline epithelial seam has to be removed to create an intact palate. This is done by a number of different mechanisms including apoptosis, epithelial to mesenchymal transformation and migration of the epithelial cells to adjacent epithelia. TUNEL (terminal deoxynucleotidyl transferase nick-end labeling) assays have identified the importance of apoptosis in the removal of the midline seam (Cuervo et al., 2002; Nawshad, 2008). The role of epithelial-mesenchymal transformation is controversial (Fitchett and Hay, 1989; Nawshad, 2008). Some believe that the epithelial cells are not transforming, but are instead migrating to the adjacent epithelia (Cuervo and Covarrubias, 2004; Xu et al., 2006). The newer genetic methods of tracing epithelial cells are better and on occasion it is possible to see labeled epithelial cells in the mesenchyme (Jin and Ding, 2006). Regardless of the mechanism, the secondary palate fusion results in removal of the epithelial seam and as a result sometimes epithelial islands remain in the midline. These epithelial remnants are thought to be the cause of midline cysts otherwise known as Bohn's nodules (Monteleone and McLellan, 1964; Saunders, 1972). The final events of fusion connect the nasal side of the secondary palate to the nasal septum and the anteriorly the palatal shelves join with the primary palate. Failure of one of the palatal shelves to fuse with the nasal septum causes unilateral cleft palate whereas failure to fuse on both sides of the septum causes bilateral cleft palate (Dixon et al., 2011)

1.3.2 Development of the hard palate in the fetal period

The hard palate is comprised of the primary palate and the anterior aspect of the secondary palate that is supported by bone. The bones of the hard palate consist of paired palatine process of the maxillary bone and more posteriorly, the palatine bones. These bones develop from intramembranous ossification, differentiating directly from neural crest mesenchyme to osteoblasts. The palatine processes of the maxilla form from de novo ossification centers that are initially separate from the maxillary bone (Bush and Jiang, 2012). The palatal processes of the palatine bones form by expansion of osteogenic fronts from the lateral aspects of the bone towards the midline (Baek et al., 2011; Bush and Jiang, 2012). When defects in the bony hard palate develop after successful soft tissue fusion, a form of submucous cleft of the palate occurs.

1.3.3 Development of the soft palate in the fetal period

The soft palate is the posterior muscular portion of the secondary palate. It has critical functions during swallowing and speech. Dysfunction in soft palate movement or ability or create a seal with the pharynx leads to velopharyngeal insufficiency, which is characterized by nasal regurgitation during swallowing, hypernasal speech, and in very severe situations, failure to thrive (Ha et al., 2013; Itani et al., 2000).

Soft palate development in humans begins after palatogenesis of the hard palate, and is generally thought to occur during weeks 9-12 of development. By 16-17 weeks, soft palate myogenesis is also complete and this is considered to be the end of palate morphogenesis (Cohen et al., 1993). Significant research has gone towards development of the hard palate, but relatively little attention has been given to the mechanism of soft palate development.

The landmark study by which most craniofacial textbooks cite the mechanism of soft palate development is from Burdi and Faist (Burdi and Faist, 1967). Their hypothesis is that after the hard palate develops by fusion of the palatal shelves, the soft palate forms through migration and proliferation of two subepithelial mesenchymal growth centers at the posterior edge of the newly fused hard palate, with groove between these structures filled in via merging (Fig. 1.1). Thus in the Burdi and Faist mechanism of soft palate development, only merging occurs and there would be no midline seam between the soft palate shelves. Their study had 31 embryos and fetuses, ranging in age from 7-12 weeks and in size from 18-75mm crown-rump length (Table 3.2). Of these specimens, ten were of the age where fusion of the hard palate would be complete, but only two were at an age where soft palate shelves are likely to have contacted but not yet fused (Table 3.2). With such a low sample size, it is not surprising that in their observations, no seam or epithelial remnants were seem in the soft palate. Furthermore, others have reported that the seam in the soft palate is subject to rapid degradation (Kitamura, 1966). Poswillo (Poswillo, 1974) also proposed a similar mechanism of soft palate development to that of Burdi and Faist in which fusion occurs in the anterior two thirds of the soft palate while

the posterior third including uvula, develops by merging. With the limited sample size in the Burdi study, it is clear that additional investigations are necessary to determine whether or not the soft palate forms by fusion or merging.

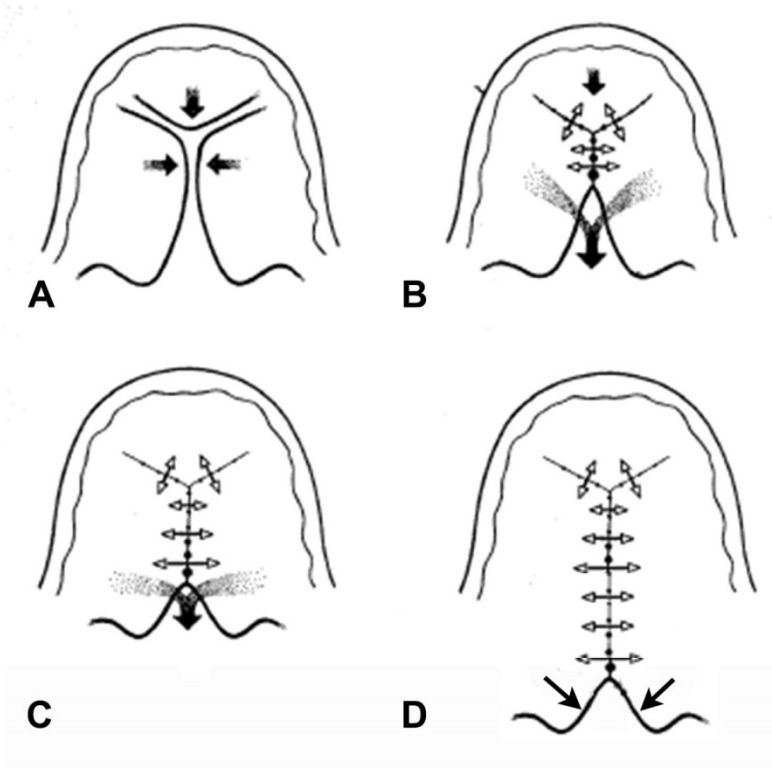

Figure 1.1. Schematic of palate closure from Burdi and Faist, 1967.

A) The primary palate grows posteriorly to meet the palatal shelves. B) Open arrows show areas of fusion with epithelial seams whereas stippled black arrow shows mesenchymal proliferation and merging. C) Continued merging of the soft palate due to mesenchymal proliferation shown by stippled black arrow. D) Fusion is still continuing anteriorly but solid black arrows show that uvula is forming via merging.

There are several additional studies that have looked specifically at the soft palate. In one study human specimens age 7-11 weeks (Wood and Kraus, 1962) were examined. In the text of the article, these authors indicated that the soft palate shelves fused but did not illustrate the seam. They directed most of their attention

to the hard palate where they observed numerous keratinized epithelial inclusion bodies, or pearls. In contrast in the soft palate no such islands of epithelium were seen. It is worth noting that the epithelium of the hard palate may have a different, ectodermal origin than that of the soft palate which is most likely derived from endoderm. The difference in origins could explain why no seam or epithelial islands were observed in the soft palate. (Sperber and Guttman, 2010). In a Japanese study, epithelial remnants have been located in the midline of the soft palate of specimens between 53-55 days post-conception but had disappeared by 60 days (Kitamura, 1966). Palatal cysts of the newborn located in the hard palate are very common (54-79% of newborns (Monteagudo et al., 2012; Paula et al., 2006). By comparison, midline palatal cysts of the soft palate are extremely uncommon . Only six case reports of epidermoid cysts requiring surgical intervention in the soft palate have been reported as of 2010 (Suga et al., 2010).

The main opponent of the Burdi work was Smiley (Smiley, 1972; Smiley, 1975; Smiley and Koch, 1975; Suga et al., 2010). He strongly believed that fusion was the main mechanism of soft palate development. He questioned how certain types of submucous clefts could develop if merging was the only process occurring, for example a perforation in the posterior hard and anterior soft palate, with intact soft palate posterior to the cleft defect (Smiley, 1972). He also believed that differential rates of midline epithelium degradation exist, with the soft palate seam forming later but degrading much more rapidly than the hard palate seam (Mato et al., 1972).

1.3.4 Muscle development in the soft palate

After seam formation and degradation the next critical event during soft palate morphogenesis is the invasion of myoblasts and formation of the palatine musculature. The palatine muscles develop from the first and fourth pharyngeal arches. The tensor veli palatini is the first palatal muscle to develop and the only one to develop from the first arch, and this is the only one to have innervation from the trigeminal nerve. It is composed of two heads, the lateral head originates on the sphenoid bone and the medial head originates at the auditory tube (De la Cuadra Blanco et al., 2012; Sperber and Guttman, 2010). When fully developed, the two heads join and wrap around the pterygoid hamulus, inserting in to the palatine aponeurosis (De la Cuadra Blanco et al., 2012). The palatine aponeurosis is a fibrous band extending off the posterior of the hard palate. It serves as point of origin and insertion for the muscles of the soft palate. For the purpose of this study, continuity of aponeurosis and tensor veli palatini can serve as a marker for completion of soft palate fusion (De la Cuadra Blanco et al., 2012).

The levator veli palatini, palatopharyngeus, musculus uvulus and palatoglossus muscles are all derived from the fourth pharyngeal arch and are innervated by the vagus nerve (Sperber and Guttman, 2010). They all develop at approximately the same time in a fetus. Failure of any of these muscles to fully develop or reach its site of insertion can result in a cleft of the muscles, which is a variant of a submucous cleft. Because of the embryologic origin of these muscles, first pharyngeal arch and fourth pharyngeal arch syndromes can exhibit submucous

clefts of the palate and velopharyngeal insufficiency (Passos-Bueno et al., 2009; Sadler and Langman, 2010a; Sperber and Guttman, 2010).

1.3. Clefting of the palate

Isolated clefts of the palate are rarer than cleft lip with or without cleft palate (CL/P). CL/P occurs in approximately 1:700 live births (Dixon et al., 2011; Mossey et al., 2009) whereas the incidence of cleft palate only (CPO) is approximately 1:1500 live births (Murray and Schutte, 2004). Even rarer are submucous clefts which are a microform of CPO. The incidence has been reported as anywhere from 1:1250-1:5000 (Garcia Velasco et al., 1988; Weatherley-White et al., 1972). The presentation of a submucous cleft ranges from bifid uvula which is often undiagnosed, to notching or defects of the bone of the posterior hard palate, to complete clefting of the muscles of the soft palate. Symptomatic clefts of the muscles of the soft palate are associated with velopharyngeal insufficiency (VPI), which prevents the soft palate from creating a seal between the oral and nasal cavities during function. This can cause difficulties with swallowing and hypernasal speech, and can lead to hearing loss due to chronic otitis media (Pauws et al., 2009b) . Often surgical intervention will be required to repair the defects in the muscles, however 30% of all clefts with soft palate defect that are operated on will have persistent VPI and hypernasal speech (Cohen et al., 1993).

1.4. Microforms of clefting

Many microforms of cleft lip have been discussed in the literature. These defects generally cause no functional impairment. Microforms of cleft lip range from notching of the upper lip, notching of the alveolar ridge +/- defects in the adjacent lateral incisor, or asymmetry in the alar cartilages (Mittal et al., 2012). Recently, occult defects in the orbicularis oris muscle have been identified as the mildest form of cleft lip microforms. Often children with non-syndromic cleft lip will have family members with notching of the orbiularis oris, at a rate of 13% (Mittal et al., 2012). When viewing defects of the orbicularis oris as a microform of cleft lip, it would be reasonable to consider the defects associated with submucous clefting of the palate such as bifid uvula, zona pellucida, and notching of the hard palate with absence of a posterior nasal spine as microforms of cleft palate (Ha et al., 2013). Furthermore, the occult submucous cleft palate patients who have velopharyngeal insufficiency with no identifiable anatomical defects (Kaplan, 1975) could be the most subtle microform of cleft palate. Generally, velopharyngeal insufficiency is due to an inability of the right and left portions of the levator veli palatini muscle to contact in the midline, and thus the muscle does not elevate the palate sufficiently during function (Weatherley-White et al., 1972). The VPI microform of cleft could be due to an intrinsic defect in the levator veli palatini. When occult submucous clefts are considered, the incidence of submucous clefting of the palate may be significantly higher than the values of 0.02-0.08% of children reported in the literature (Weatherley-White et al., 1972). Furthermore, identification of families with submucous clefts may predict individuals who are more likely to have children born with cleft palate.

1.5. Etiology of orofacial clefting

The etiology of clefting is multifactorial, having both genetic and environmental influences (Beaty et al., 2011; Marazita, 2012), however it is thought that CPO has a larger genetic contribution. 1.3-25.3 in 10,000 infants will be born with cleft palate only and as many as 61% of cleft palate only patients have other developmental abnormalities that could be part of a syndrome (Bell et al., 2013; Mossey and Castilla, 2003). Isolated cleft palate occur more frequently in females than males (Mossey and Little, 2002).

There are environmental factors that increase the risk of human orofacial clefting. These include teratogens as well as such factors as smoking, alcohol, maternal obesity (Dixon et al., 2011). The animal studies on teratogens causing cleft palate were recently reviewed by Barbara Abbott (Abbott, 2010) . Cortisone was shown to induce cleft palates in mice in a dose-dependent manner (Fraser and Fainstat, 1951; Fraser et al., 1954). Cortisone exposure lead delayed elevation of the palatal shelves and failure to contact and fuse (Diewert and Pratt, 1981; Kalter and Warkany, 1961). Vitamin A (retinoic acid) exposure in rats produced a number of congenital anomalies including cleft palate (Cohlan, 1953; Kalter and Warkany, 1961; Walker and Crain, 1960). The palatal shelves of offspring of rats exposed to vitamin A were small and abnormal in size, and failed to contact in the midline. Other teratogens cause cleft palate by impeding growth of the mandible. In such a scenario palatal shelves will remain lodged beside the tongue and will not reorient at the correct time (Diewert, 1981).

The anti-seizure medication Dilantin increases the risk of clefting. In a mouse study, submucous clefts were induced by exposing the pregnant mothers to high doses of oral phenytoin (Poswillo, 1974). The control and experimental offspring developed in a similar fashion until the time period between days E16.5-E18.5. At this point the ossification centers of the palatal process of the maxilla were extending medially in to each palatal shelf, however in the experimental group, the plates failed to extend all the way to the midline, and thus never contacted to create a midpalatal suture in the hard palate. Similar findings were seen in the soft palate, as there was no uvula in the experimental group and the soft palate was much thinner than the control group, representing a midline deficiency. None of the experimental groups had bifid soft palates, ie all palates fused, the clefts were only submucous. Thus in the case of seizure medications, there may be a specific risk of inducing soft palate clefting.

There is also an important genetic component to the etiology of clefting. Multiple genes are likely to be involved, some of which will have mutations that lead to a change in function and others that may have subtle sequence variations that do not obviously change protein function or expression. To attack the complex nature of human clefting studies have used candidate gene approaches exploring the variation in genes known to cause human craniofacial syndromes or mouse facial phenotypes.

Two syndromic genes that have been studied in isolated clefts (non-syndromic) are the transcription factors *IRF6* (interferon regulatory factor 6) and *TBX22* (T-box transcription factor). *IRF6* is mutated in Van der Woude's syndrome (Kondo et al., 2002) whereas *TBX22* is mutated in X-linked cleft palate ankyloglossia (Braybrook

et al., 2001). In the case of IRF6, numerous studies link variation in the gene with non-syndromic clefting (Park et al., 2007; Scapoli et al., 2005; Zucchero et al., 2004). *TBX22* mutations have been associated with non-syndromic isolated cleft palate (Marcano et al., 2004; Suphapeetiporn et al., 2007). Additional genes that have been associated with non-syndromic CPO include *FOXE1*, *MSX1*, and *SATB2* (Bush and Jiang, 2012). These genes are involved in various stages of secondary palate development and gene targeting experiments have been shown to cause clefting in mice.

More recently unbiased, genome-wide association studies (GWAS) have been performed to identify additional variants associated with non-syndromic orofacial clefting (Marazita, 2012). To date, four studies have been performed on CL/P cases and controls (Beaty et al., 2010; Birnbaum et al., 2009; Grant et al., 2009; Mangold et al., 2010) and one on CPO cases and controls (Beaty et al., 2010; Beaty et al., 2011). The first CL/P of this kind identified IRF6 as a causative gene in CL/P (Birnbaum et al., 2009). This study as well as others have linked CL/P to sequence variations on chromosome 8q24 which as yet is considered to be a gene desert (Beaty et al., 2010; Beaty et al., 2013). Two additional loci were found, at 17q22 near NOGGIN and 10q25.3 near VAX1 (Mangold et al., 2010). One of these studies examined gene-environment interactions and found that while no polymorphism reached significance on its own there were several that when combined with alcohol exposure or smoking increased risk of cleft palate (Beaty et al., 2011). Thus clefting remains a complicated disorder that may be difficult to tease apart. Nevertheless

some of the environmental risk factors could translate into recommendations for pregnant women.

1.6 Aims

The primary aims of my study are:

1) To analyze soft palate development on a more representative group of human specimens than what was used by Burdi and Faist (Burdi and Faist, 1967)

2) To observe the presence or absence of midline epithelial seams between the soft palate shelves during development.

3) To assess the invasion of soft palate muscles in relation to the midline seam.

Chapter 2 - Methods

2.1. Preparation of specimens and processing into paraffin

The specimens obtained for this study were stored in the lab of Dr. V. Diewert either as paraffin sections or as specimens stored at 4°C. These non-processed specimens were stored in 4% paraformaldehyde since 1988.

Specimens obtained in 4% PFA were washed twice in PBS for one hour each, photographed at multiple angles using a Leica stereoscope. To facilitate sectioning, it was essential to decalcify the osseous tissue. In some archival material already embedded in paraffin and sectioned there was evidence of tearing of tissues due to incomplete decalcification.

All specimens were transferred into 7% EDTA and placed on a shaker at 4˚C. This decalcification solution was changed every 2-3 days for 8 weeks. Once it was determined that no additional bone remained in the specimens by piercing non-critical regions of the skull with a pin, they were washed twice in PBS for one hour each, then 50%PBS/50%EtOH for one hour, then 70% EtOH in water. They were then processed into wax blocks at the UBC Department of Histopathology. The specimens were remelted in the lab and repositioned within the molds to ensure even transverse sections could be obtained. All specimens were sectioned at thickness of 7μm on a microtome. Sections were placed on TESPA-coated slides so that they could be used for molecular studies.

2.2. Histochemical and immunohistochemical staining procedures

Picrosirius red and Alcian blue staining

Sections were dewaxed in two washes of xylene for 20 minutes each, 100% EtOH for 2x10 minute, 90% EtOH for 5 mintues, 70% EtOH for 5 minutes, 50% EtOH for 5 minutes and ddH_2O for 5 mins. First Alcian blue staining was performed by immersing sections in 1% alcian blue in acetic acid for 30 minutes followed by 1% acetic acid for 5 mins, ddH_2O for 5 mins. Next the sections were counter stained with Picrosirius red for 1 hour in the dark, 1% acetic acid for 5 min, and ddH_2O for 5 min. Specimens were rehydrated in the opposite order as they were dewaxed, then mounted on slides using Entellan mounting medium.

Hematoxylin and Eosin staining

The dewaxing protocol was performed in the same manner as Picrosirius red and Alcian blue staining. Slides were then stained in Shandon hematoxylin for 5-7 minutes, ddH_2O for 5 minutes, immersed in in saturated lithium carbonate solution for 1 minute to blue the hematoxylin, dipped in 1% Eosin Y aqueous solution 30 times and rinsed in ddH_2O for 5 minutes. Specimens were dehydrated in the opposite order as they were dewaxed and coverslipped as described above.

Immunohistochemistry protocol for MF20 muscle antibody

The MF20 mouse monoclonal antibody was obtained from the Developmental Studies Hybridoma bank. This antibody is raised to chicken myosin and cross reacts with a wide variety of species. Sections were dewaxed, rehydrated to 50% ethanol and rinsed in PBS three times for 2 minutes each. A Proteinase K treatment was performed for 10 minutes at 37° C using 5μg/ml in Proteinase K buffer. Sections were rinsed again in PBS three times. Blocking was performed with 1%BSA, 0.02% TWEEN and 1% sheep serum for 30 minutes at room temperature in a humidified chamber. The MF 20 primary antibody (supernatant) was added undiluted to the sections and left for one hour at 37°C. It was then rinsed in PBS again three times. The secondary antibody used was anti-mouse IgG biotinylated antibody 1:500 in PBS and 0.2% BSA (ABC kit, Vector Labs) and was added to the sections for one hour at room temperature. Again sections were rinsed three times in PBS. From the ABC Kit, 1 drop of A and 1 drop of B were added to 3.2mL PBS 30 minutes before needed for use, then incubated with the sections for one hour at room temperature. DAB detection was performed in the dark at room temperature. The detection solution (200μL 50x DAB and 10mL 1x DAB buffer) was applied to slides and reaction was monitored. The detection solution was left on slides for 10-20 minutes until a full reaction was observed. The reaction was stopped by washing in water three times for one minute each, then washed in distilled water for 5 minutes. Conterstaining was done with Picrosirius red and Alcian blue and slides were prepared as per above protocol.

2.3. 3D reconstruction of human fetuses at various stages of palatogenesis

Thirteen sectioned and stained human specimens at 54-74-days of development were photographed serially at the hard-soft palate junction on a Zeiss Axiophot compound microscope. These high resolution images were imported in to WinSurf 3D Reconstruction program (SURFdriver Software, Kailua, HI, USA developed by Scott Lozanoff). The structures of interest included the hard palate, soft palate, palatine bones, midline epithelial seam, palatine aponeurosis, and the nasal septum. These structures were traced on the sequential photos for each specimen. The tracings were then stacked together to create the reconstructed structures. The stacks were aligned within the Winsurf program and smoothed to create a representation of the hard-soft palate junction. Screen captures were created from different views of the reconstruction and imported into Adobe Photoshop.

Chapter 3: Results

3.1. Overview of craniofacial development from 54 – 74-days post conception

In order to gain an overview of the morphogenesis of the human head I will describe the major structures that are developing at each stage of development encompassed in my sample. The bones, cartilages, teeth, muscles and salivary glands are all present in the specimens and help to provide another measure of the state of development in addition to the stage of palate closure. The specimens collected had crown rump lengths ranging from 35 to 75 mm (data obtained from U of Washington, Table 3.1, 3.3). The stages I examined cover those included in the Burdi study but expand the numbers in 41-70 mm CR length which is the critical period covering soft palate fusion (Table 3.2). Sex information for the individual specimens was not available.

Table 3.1 Palate development in individual human embryos and fetuses

Specimen number	Days post conception	Crown-rump length (mm) as per UW	Hard palate (fused with seam, seam has epithelial remnants, no seam fully fused)	Soft palate (not fused, partially fused with seam, fused with seam, fused with aponeurosis)		
			Posterior	Anterior	Middle	posterior
H7832	54d	35	Fused with seam	Fused with seam	Partially fused with seam	Not fused
H9978	54d	35	Fused with seam	No sections in soft palate, excluded from sample		
H9517	57d	41	Fused with seam	Partially fused with seam	Partially fused with seam	Not fused
H10142	57d	41	Fused with remnants of seam	Fused with remnants of seam	Fused with remnants of seam	Not fused
H10458	57d	41	Fused with seam	Fused with remnants of seam	Fused with remnants of seam	Not fused
H11032	57d	41	Fused with seam	Fused with remnants of seam	Partially fused with seam	Not fused
H10593	59d	42	Fused with seam	Not fused	Not fused	Not fused
H9652	59d	42	Fused no seam	Fused no seam, developing aponeurosis	Fused no seam, developing aponeurosis	N/A
H9854	64d	43-62	Fused with remnants of seam	Fused no seam, developing aponeurosis	Partially fused with seam	Not fused
H10071	67d	63	Fused with remnants of seam	Fused no seam, developing aponeurosis	Fused no seam, developing aponeurosis	Not fused
H9705	70d	64-68	Fused with remnants of seam	Fused no seam, developing aponeurosis	Fused no seam, developing aponeurosis	Fused with seam
H9832	70d	64-68	Fused with remnants of seam	Fused with aponeurosis	N/A	N/A
H9819	74d	75	Epithelial pearls	Fused with aponeurosis	Fused with aponeurosis	Fused with aponeurosis

Table 3.2 Comparison of crown-rump length of specimens from current study with Burdi and Faist 1967 study

Crown-rump length (mm)	My study (n=)	Burdi and Faist (n=)
35-40	2	7
41-60*	6	2
61-70*	4	0
71-75	1	1

* Key stages of soft palate seam formation

3.1.1 Tooth development

The stages of individual tooth development pass through initiation, morphogenesis, histodifferentiation and eruption. The enamel of teeth is formed from ectoderm, and the dentin and pulp are made from ectomesenchyme of neural crest origin. The communication between these two layers is critical for regulating the signaling mechanisms involved in tooth development (Jussila and Thesleff, 2012). Tooth development with dental lamina formation early as 28 days pc, and root development continues until 3 years post-eruption (Ooë, 1981). Initially, teeth begin as dental placodes, which are localized epithelial thickenings within the dental lamina. In the specimens studied here teeth reach bud, cap and bell stage. In the 54 and 57-day specimens there are some bud and cap stage teeth (Fig. 3.1A,B). In the 64, 67 and 70-day specimens there are teeth at bud, cap and early bell stage (Fig. 3. 1C,D,E,E'). At no time was histodifferentiation observed.

3.1.2 Cartilages

The vertebrate skull is divided into three main parts: the splanchnocranium visceral skeleton), the dermatocranium (membranous bones) and the chondrocranium. The chondrocranium, or neurocranium, is the primitive skull that is evolutionarily conserved amongst all vertebrates (Sperber and Guttman, 2010).

The function of the chondrocranium is to support the brain and sensory organs of the skull. In cartilaginous fishes, the chondrocranium will persist as cartilage, however in bony fishes and higher vertebrates the cartilage of neural crest origin will ossify by endochondral ossification. The bones of the chondrocranium in humans make up the cranial base (Sadler and Langman, 2010b). In the present study it is possible the entirety of the nasal capsule including turbinates, septum and ethmoid (Fig. 3.1A-E). The orbital cartilage and Meckel's cartilage are also differentiated (Fig. 3.1A-E).

3.1.3 Bone development

The majority of the bones of the face and cranial vault develop by purely intramembranous formation (frontal, parietal, nasal, lacrimal, zygomatic, vomer, palatine and maxilla)(Sperber and Guttman, 2010). Others develop through purely endochondral formation (incus, stapes, ethmoid inferior concha and hyoid). The remaining craniofacial bones develop by a mixed endochondral-intramembranous combination (maleus, temporal, sphenoid, mandible and occipital).

Even in the youngest 54-day specimen, there is a significant amount of ossification. The palatine processes of the maxilla are ossifying. Ossification of the mandibular bone is occurring around Meckel's cartilage. The transverse portion of the frontal bone making up the superior orbital wall has also undergone significant

ossification and the paired ossification centers of the vomer are present. By 70-days the majority of the facial bones are present (Fig. 3.1A-E).

3.1.4 Muscle development

There are approximately 60 muscles in the human head, which are crucial to our ability to move the head, swallow, and move our eyes. The voluntary muscles of the head and neck develop from the somitomeres and somites which are composed of paraxial mesoderm (Sperber and Guttman, 2010). The extraocular muscles are the first to form and begin to develop at 3-4 weeks post conception (Sevel, 1981). Extraocular muscles arise from mesoderm in three different centers of development, based on the cranial nerves that innervate them: one for the muscles that are innervated by cranial nerve III (oculomotor): superior, medial and inferior rectus and the inferior oblique, and separate areas for the superior oblique (CN IV) and lateral rectus (CN VI) (Gilbert, 1952). The medial rectus, superior oblique, inferior rectus are present in 54-day specimens (Fig. 3.1A).

The other muscles that are present at 54-days include the masseter, tongue, myelohyoid and anterior belly of the digastric (Fig. 3.1A). Some of these muscles were already forming in the head during the embryonic period. For example, the muscles of the tongue (except for the palatoglossus) migrate into the tongue swellings beginning at 5 weeks (Sperber and Guttman, 2010). The origins of the tongue musculature are the pharynx at the level of the occipital somites.

The muscles of mastication include the temporalis, masseter, pterygoids, anterior belly of the digastric, mylohyoid, tensor veli palatini and tensor tympani. With the exception of the TVP, muscles of mastication develop before the muscles of the soft palate (Sperber and Guttman, 2010), but after the development of the mandible has begun (Cohen et al., 1993). Their origin is the first pharyngeal arch, thus they receive innervation from the mandibular branch of the trigeminal nerve (Sadler and Langman, 2010b)

The tongue is also prominent in all stages examined in my study. This is not surprising since the tongue initiates during the fourth weeks as lingual swellings from the first arch (Sperber and Guttman, 2010).

The muscles of the soft palate originate from mesenchymal tissue of the first and fourth arches (Sperber and Guttman, 2010). By 16-17 weeks, the full postnatal soft palate musculature is developed (Cohen et al., 1993). The first soft palate muscle to invade the palatal shelf mesenchyme is the tensor veli palatini at 40 days pc. Next is the palatopharyngeus at 45 days, the levator veli palatini during the 8th week, while the palatoglossus and the musculus uvulus are the last to form during the 9th week (Cohen et al., 1993; De la Cuadra Blanco et al., 2012; Katori et al., 2011; Rood, 1973; Seif and Dellon, 1978; Sperber and Guttman, 2010). The palatoglossus does not attach to the soft palate until the 11th week, as it originally develops with the muscles of the tongue (Sperber and Guttman, 2010). Therefore all of these muscles are forming in our 54-day specimen (Fig. 3.1A and data not shown). The tensor veli palatini muscle migrates to the precursor to the palatine aponeurosis during the 8th week. By the 9th week, the tensor veli palatini is continuous with the

aponeurosis (De la Cuadra Blanco et al., 2012). More focused descriptions of the soft palate including seam formation, invasion of soft palate muscles and insertion of muscles into the aponeurosis follows in subsequent sections of the results (Figs. 3.2-3.5,3.7).

I conclude that the specimens I am studying are grossly consistent with data from others for the equivalent stages of development.

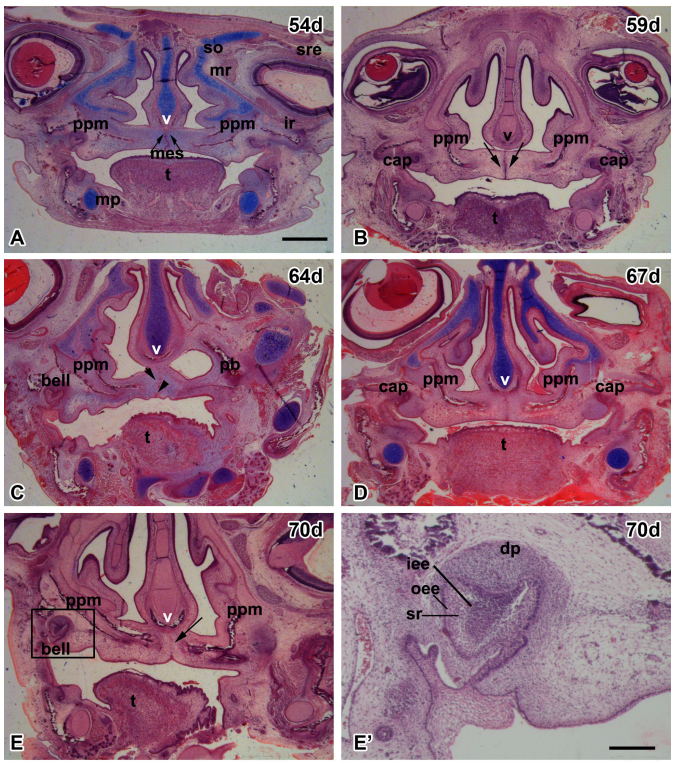

Figure 3.1. Overview of craniofacial development in the conceptuses used in this study.

Frontal sections of human fetuses at different stages of development, sectioned through the posterior hard palate. A) A specimen stained with Picrosirius Red and Alcian Blue. The shelves of the hard palate are fusing in the midline and the presence of a continuous midline epithelial seam is observed (arrows). The hard palate has already fused with the nasal septum. Cartilages and intramembranous bones have differentiated in the upper and lower jaws. The extraocular and tongue muscles are present. A maxillary right primary molar is seen in the bell stage of development while the other three primary molars are in cap stage. B) A specimen stained with hematoxylin and eosin. The palatal shelves have contacted in the midline and a continuous seam is present between the palatal shelves (arrows). The attachment of the shelves to the nasal septum appears tenuous with a continuous epithelial layer separating the structures. Similar cartilage, bone and muscle development is seen as in the 54-day specimen, however the masseter muscles can now be. Two bud stage molars can be seen developing in the right and left maxillae. C) A specimen stained with Picrosirius Red and Alcian Blue. The seam in the hard palate is beginning to break down and shows collections of epithelial cells (black arrowheads) There is increased ossification compared to younger specimens. D) A specimen stained with Picrosirius Red and Alcian Blue. The medial edge epithelium between the palatal shelves is degrading, with islands remaining at the superior and inferior aspects of the fusing shelves. The palatine process of the maxillary bone is infiltrating the hard palate. Cap stage teeth are seen on both sides of the maxilla. E) A specimen stained with hematoxylin and eosin which was cut at an angle. The medial edge epithelium is almost completely degraded, with a few epithelial remnants persisting in the oral side of the midline seam of the hard palate (arrows). A primary tooth in bell stage is seen in the upper right maxilla (black box). F. Area inside the black box of E. This enamel organ and dental papilla of the primary molar are clearly visible but no dentin or enamel has been deposited. The successional lamina of the developing premolar is also visible lateral to the developing primary molar. Key: bell – bell stage tooth bud, cap – cap stage tooth bud, dp – dental papilla, iee – inner enamel epithelium, ir - inferior rectus, mes – midline epithelial seam, mp - medial pterygoid, mr – medial rectus, oee – outer enamel epithelium, ppm – palatine process of the maxilla, so – superior oblique, sr – stellate reticulum, sre – superior rectus, t – tongue, v – vomer. Scale bar =1mm for panels A-E and 200 µm.

3.2. Palate development according to stage of embryo

3.2.1 54-day specimens have incomplete fusion of the hard and soft palates

The embryonic period is nearly complete by 54-days gestation. The primary palate has fully fused by 47 days (Ooë, 1981), the palatal shelves have reoriented across the oral cavity and are undergoing fusion with the primary palate. The shelves have contacted and largely completed fusion in the hard palate, however the epithelial seam may still be present. Two 54-day specimens were examined (Table 3.1, 3.3). The region from the posterior hard palate to the termination of the soft palate were examined. The Atlas of Developmental Anatomy of the Face (Kraus et al., 1966) was used to accurately determine when the transition from soft to hard palate occurred. The eyes, optic nerves and nasal septum were used to determine the depth of the sections. Other landmarks included the transition from a vertical orientation of the palatal nerve to a horizontal position as it enters the soft palate, and the presence or absence of horizontal palatine bones in the palatine shelves. One specimen (Figure 3.1) was intact but the other was lacking the majority of the soft palate (data not shown, H9978). In the intact specimen a midline seam is present in the hard palate but is mostly degraded with thickened epithelium on the superior and inferior aspects (Fig. 3.1A,A'). Some epithelial remnants are present in the centre of the hard palate (Fig. 3.1A'). In the soft palate, the shelves have made contact and an epithelial seam runs through the midline (Fig. 3.1B,B'). The same thickened areas of epithelium exist on the nasal and oral aspects. Mesenchymal condensations lateral to the midline represent the developing palatine aponeurosis.

The posterior soft palate (C) exhibits a lobular shape, most likely due to the curve of the soft palate as it projects down towards the uvula. The midline epithelium is thicker and more irregular in this region. It is not possible to see the developing aponeurosis in this region, but distinct lateral condensations in the soft palate shelves represent the developing tensor veli palatine muscles. It is not possible conclude based on the single specimen whether the extent of fusion of the soft palate is representative for this stage

Table 3.3 Fusion status of the hard and soft palate in University of Washington specimens

Hard Palate				
	Seam	**Epithelial remnants**	**No seam remaining**	
54d (n = 2)	2	0	0	
57d (n=4)	3	1	0	
59d (n=2)	1	0	1	
64d (n=1)	1	0	0	
67d (n=1)	0	1	0	
70d (n=2)	0	2	0	
74d (n=1)	0	0	1	
Soft Palate				
Days post conception	**Not fused**	**Partially fused with seam**	**Fused with seam**	**Fused with aponeurosis**
54d (n=1)	0	1	0	0
57d (n=4)	0	1	3	0
59d (n=2)	1	0	0	1
64d (n=1)	0	1	0	0
67d (n=1)	0	0	0	1
70d (n=2)	0	0	1	1
74d (n=1)	0	0	0	1

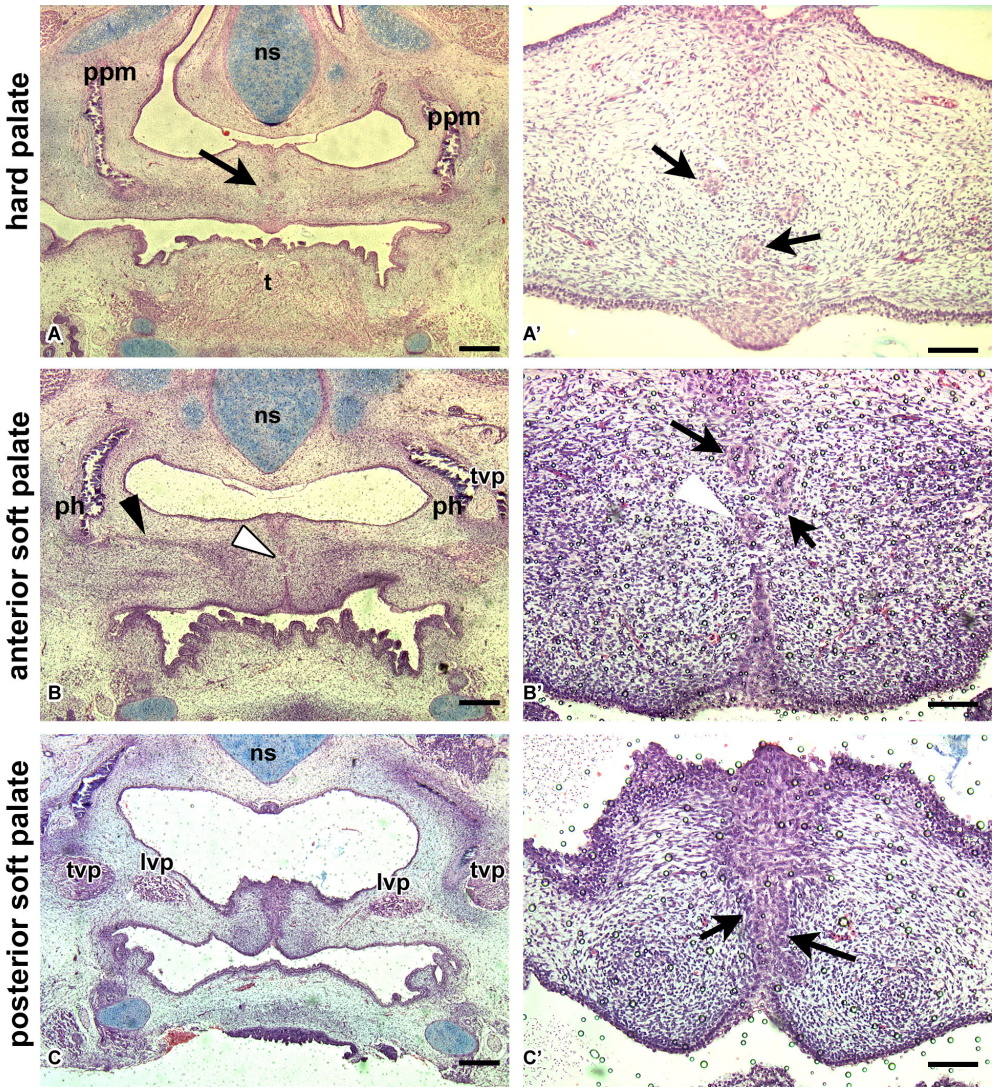

Figure 3.2. Palate morphogenesis in a 54-day specimen.

Frontal sections of a 54-day specimen beginning in the posterior hard palate and ending at the posterior soft palate stained with Picrosirius Red and Alcian Blue, Overall this specimen is precocious in its palate development. At the posterior edge of the hard palate (A, A'), the midline seam is still intact on the inferior and superior aspects, but is degrading in the centre (arrows). In the anterior soft palate (B, B'), the midline palatal seam is visible on the oral and nasal surfaces aspects. The intact regions of the seam are much bulkier than in the hard palate. Epithelial islands (white arrowhead) are present in the middle of the seam. The palatine aponeurosis is seen condensing within the right and left palatal shelves (black arrowhead). In the posterior soft palate (C, C'), the midline palatal seam is thicker than in more anterior regions. The epithelium is multilayered and poorly organized on the nasal side while on the oral side the epithelium is thinner and stratified. The staining of the basement membrane region is indistinct.The levator veli palatini muscles can be seen developing within the soft palate shelves, lateral to the seam. Even more laterally, at the base of the pterygoid hamulus, the tensor veli palatini muscles are developing and in this specimen appear very defined and robust. Key: lvp – levator veli palatini, ns – nasal septum, ppm – palatine process of the maxilla, t – tongue, tvp – tensor veli palatini. Scale bar for A,B,C =300μm; A', B', C', =100μm.

3.2.2 57-day specimens have completed hard but not soft palate closure

By 57-days, the fetal period has begun. During the fetal period the tissues and organs of the body mature, and the fetus experiences rapid growth (Sadler and Langman, 2010b).

In my study there were four 57-day specimens collected (Fig 3.3 and 3.4 and data not shown H10142 and H10458). The four 57-day specimens examined had fairly similar development in that all had completed hard palate fusion but the uvula had not formed (Tables 3.1, 3.3). In all specimens a few epithelial remnants of the epithelial seam are present (Fig. 3.3, Fig 3.4). Surprisingly, the 57-day specimens exhibited less advanced soft palate development than the more mature 54-day specimen (Fig 3.1). This suggests that the 54-day embryo was precocious. In one 57-day specimen there is almost a continuous midline seam in the hard palate (Fig. 3.3A). The middle of the soft palate (Fig. 3.3B) has an intact midline seam, with a prominent epithelial thickening or triangle on the oral side. Condensations in the middle of the shelves may indicate presence of the early palatine aponeurosis. Lateral to this, areas of the developing tensor veli palatine can be seen directly below the palatine bones (Fig. 3.3C,C'). The most posterior part of the soft palate is not contacting in the midline (Fig. 3.3C,C'). In a second 57-day specimen (Fig. 3.4) also has a continuous midline seam through the hard palate (Fig. 3.3A). The seam increases in thickness as it transitions from the superior nasal side of the palate to the inferior oral side of the palate. The anterior soft palate section (Fig. 3.4B) has a prominent midline seam, with small epithelial islands lateral to the midline (Fig.

3.4B'). Generally, the epithelial seam in the soft palate is thicker and less uniform than that seen in the hard palate (Fig. 3.3B). In the posterior soft palate (Fig. 3.4C), there is contact between the right and left palatal shelves but a thin epithelial bridge persists between the two sides. The oral surface epithelium is consistently much thicker and more irregular in appearance than that of the nasal surface. Although I did not use a specific stain for basement membrane it is generally harder to distinguish the basement membrane region from the underlying mesenchyme in the soft palate than in the hard palate (Fig. 3.3B',C'). The tensor veli palatini muscle can be seen on the right side below the palatine bone. In the terminal soft palate (Fig. 3.4D), the two shelves have not yet contacted, and they are fairly small in size..

In summary, at 57-days the soft palate has started to fuse but is incomplete in the area of the uvula. Importantly there is clear evidence for a midline epithelial seam in the soft palate at 57-days. The invasion of the tensor veli palatini has started and the aponeurosis is also beginning.

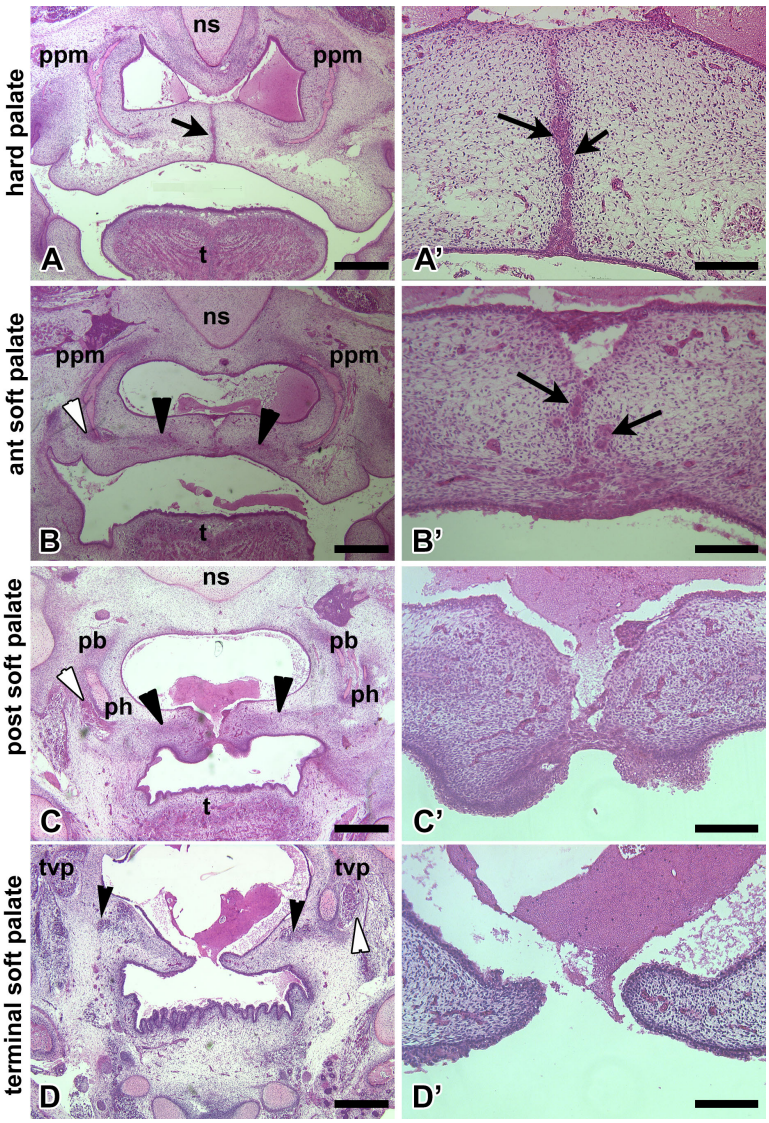

Figure 3.3 Development of the palate in a 57-day fetus.

Frontal sections stained with hematoxylin and eosin, At the posterior edge of the hard palate (A, A'), the shelves have fused and the darkly stained seam between the palatal shelves is fully intact with no regions of degradation (arrows). In the anterior soft palate (B, B'), the palatal shelves have also contacted and fused, the seam is breaking down, with multiple islands of epithelium (arrows). The palatine aponeurosis is seen condensing in both the right and left palatal shelves (black arrowheads). A small portion of the developing tensor veli palatini muscle is present in the right palatal shelf (white arrowhead). In the posterior soft palate (C, C'), initial contact has been made between the palatal shelves. A bridge of epithelium represents the initial point of fusion between the shelves. Thick layers of epithelium (C') can be seen on the oral side off the pre-fusion soft palate shelves. Note the indistinct staining of the epithelium compared to the mesenchyme.The aponeurosis is seen condensing in the right and left soft palate shelves (black arrowheads), and the tensor veli palatini is seen on the right side (white arrowhead) developing by the pterygoid hamulus. In the terminal soft palate (D, D'), the soft palate shelves have not yet contacted. These shelves are extremely small and thin compared to the fused shelves, indicating that they still need to grow in order to complete development. The left tensor veli palatini (white arrowhead) is seen in this section, as are the right and left levator veli palatini muscles developing within the soft palatal shelves (black arrowheads). Key: ns – nasal septum, pb – palatine bone, ph – pterygoid hamulus, ppm – palatine process of the maxilla, t – tongue, tvp – tensor veli palatini. Scale bar =525 μm for A,B,C,D; bar = 200 μm for A', B', C',D'.

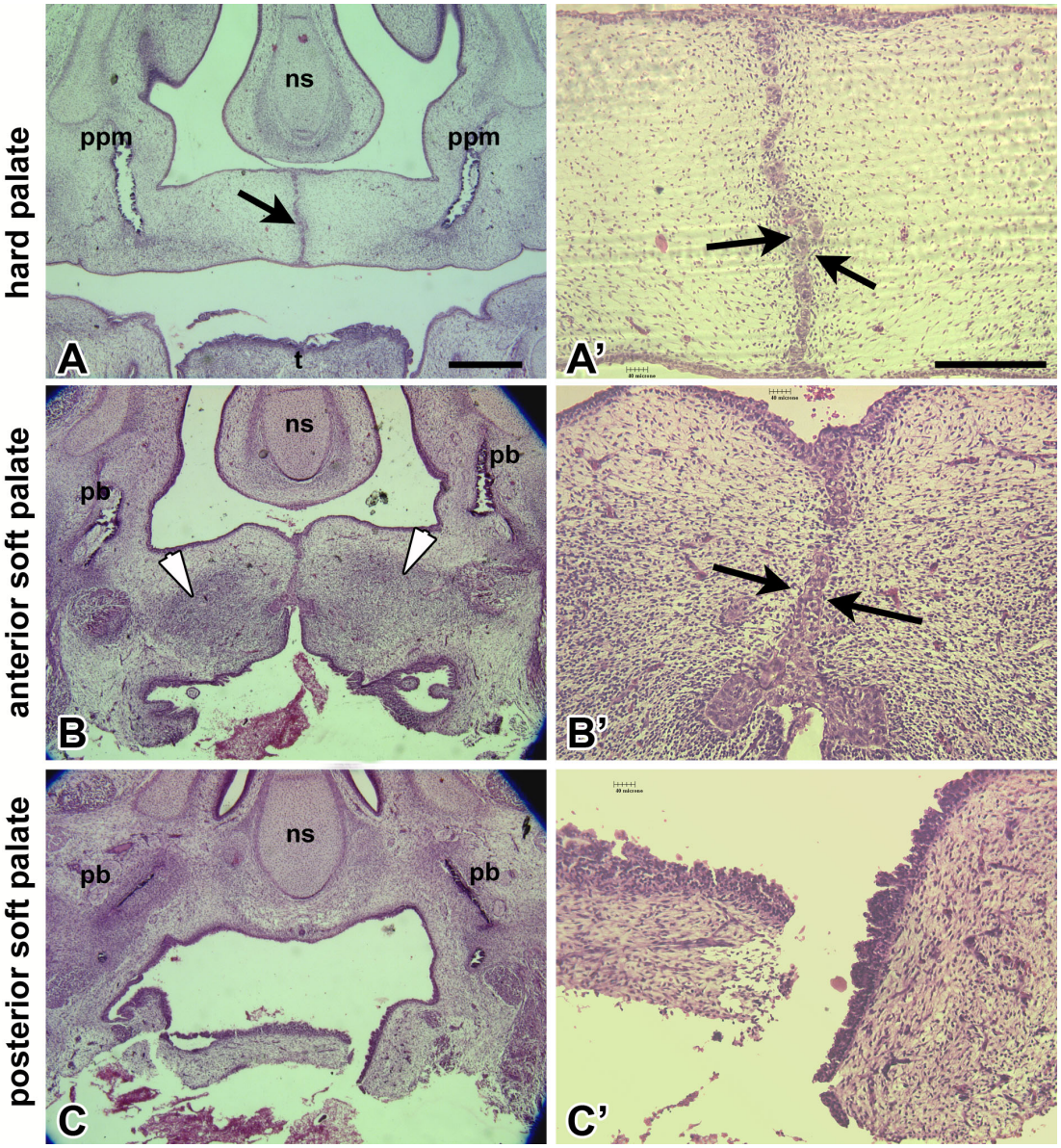

Figure 3.4 Palatal morphogenesis in a second 57-day specimen

Frontal sections of a second 57-day specimen stained with Hematoxylin and Eosin, At the posterior edge of the hard palate (A, A'), the palatal shelves are fully fused to each other and to the nasal septum. There is a bilayered seam present between the right and left palatal shelves, which is only in the initial stages of breaking down (arrows). There are small areas of epithelium the seam that appear to be more mesenchymal in appearance (black arrowheads). In the anterior soft palate (B, B'), the soft palate shelves have contacted in the midline of the superior aspect of the shelves. The midline seam between the shelves is intact and appears of mostly uniform thickness. Inferior to the base of the seam, the soft palate shelves have not yet contacted and are still open. Early condensations of the left and right palatine aponeurosis can be seen in these anterior soft palate shelves (white arrowheads). The tensor veli palatini is the only palatine muscle that can be seen developing in this section. In the posterior soft palate, (C, C'), the section has torn through the shelves, but it appears that the shelves in this aspect of the soft palate had not yet contacted. Thick epithelium lining the shelves can be seen on the nasal side of the shelves. The oral side epithelium has mostly torn off this specimen. Key: ns – nasal septum, pb – palatine bone, ppm – palatine process of the maxilla, t – tongue. Scale bar =525μm for A,B,C; bar = 200 μm for A', B', C'.

3.2.3 59-70-day specimens have complete hard palates, variable soft palate development

The two 59 day specimens examined were greatly varied in their degree of development . One exhibits complete development of the soft palate and development of the aponeurosis (Table 3.1, 3.3, H9652), while the other has a developed hard palate but the soft palate is only partially formed similar to the 57-day specimens (Fig. 3.7A-C, H10593). The more advanced 59-day specimen is similar to the 70-day specimens leading me to conclude that this particular specimen is not representative.

Further evidence to say that the typical 59 day fetus has a partially fused palate comes from the examination of 64 and 67-day specimens. In the 64-day specimens a few epithelial remnants of the epithelial seam in the hard palate are present (Fig. 3.4A). The horizontal processes of the palatine bones are extending towards the midline and the nasal septum is continuous with the nasal side of the palatal shelves. The anterior and middle soft palate sections show complete degradation of the midline seam (Fig. 3.5B,B'), however the seam is evident in posterior sections (Fig. 3.5C,C'). The posterior seam consists of thickened epithelium on the oral side. In the posterior sections, the mesenchymal condensations for the developing palatine aponeurosis are visible (Fig. 3.4C). . The 67-day specimen (Fig 3.7 D-F and Table 3.1, 3.3) has a fused soft palate with no seam present, until the posterior aspect which is still unfused. By this point, the aponeurosis is more robust

in the anterior and mid soft palate (Fig 3.7 D,E insets) and has almost connected in the midline.

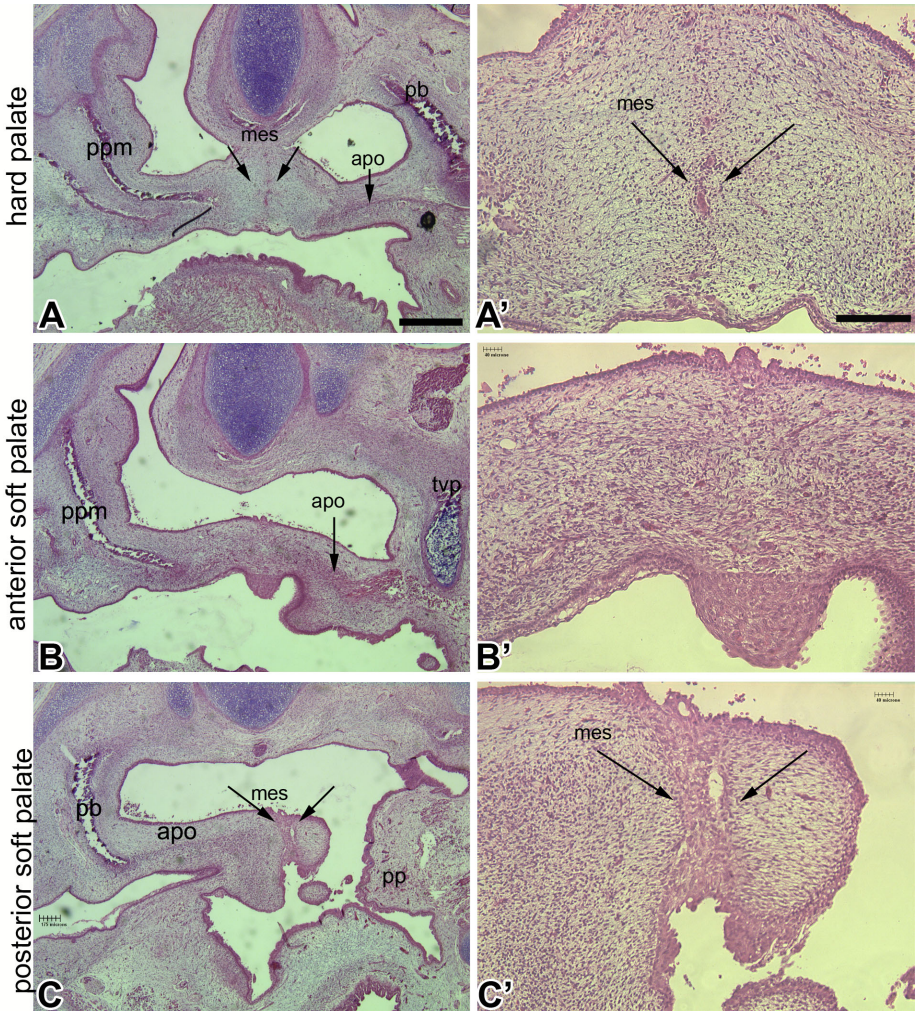

Figure 3.5. Palatal morphogenesis of a 64-day fetus.

Frontal sections through the palate stained with Picrosirius Red and Alcian Blue, This specimen was tiled so that the right side is more anterior than the left side. At the posterior edge of the hard palate (A, A'), the palatal shelves have fused. There are remnants of a midline seam in this region of the hard palate. The palatine bone is extending in to the hard palate on the right side. The anterior soft palate (B, B') is fused in the midline, with no remnants of midline seam remaining. The epithelium on the inferior aspect of the midline of the palate is thick but regular in its appearance. The palatine aponeurosis and levator veli palatini are visible in the left side of the palate. The sectioning bias of this specimen is evident in the posterior soft palate (C, C'), as the right side of the soft palate displays a full right shelf, that has contacted and fused with part of a left shelf, with a full midline seam present between the shelves (C'). The staining of the seam is very light and similar in colour to the mesenchymal stain.The aponeurosis is also present throughout the right shelf. On the lateral aspect of the left side, the more posterior developing palatal shelf is seen as a dome shaped outgrowth from the lateral pharyngeal wall. Cells of the developing palatopharyngeus muscle can be seen in this structure. Key: apo – aponeurosis, mes – midline epithelial seam, ns – nasal septum, pb – palatine bone, ppm – palatine process of the maxilla, tvp – tensor veli palatini. Scale bar in A=525μm applies to A,B,C; bar in A' = 200 μm applies to A', B', C'.

There were two 70-day specimens but unfortunately only one of these included the full soft palate (data not shown, H9705). The other was missing tissue posterior to the junction of the hard and soft palate and was uninformative (data not shown, H9832). The intact specimen had full fusion of the soft palate and only the uvula retained part of the epithelial seam. This specimen provided convincing evidence for a model of fusion of the entire soft palate from the anterior aspect to the tip of the uvula, contradicting a previous theory of fusion of the anterior 2/3 of the soft palate and merging of the uvula (Poswillo, 1974). Interestingly, the hard palate retains numerous midline epithelial islands well into the fetal period and beyond whereas the seam in the soft palate is much more transient.

3.2.4 74-day specimen has a fully developed soft palate and aponeurosis

The only 74-day specimen obtained was sectioned in the coronal plane or in the same plane as the palate itself (data not shown, H9819, Table 3.1.3.3). This is the only specimen in my study in which the, soft palate is fully formed as shown by the complete absence of epithelial islands or a seam in the midline mesenchyme.The aponeurosis is continuous across the soft palate and the tensor veli palatini muscles have attached to its distal ends. . As noted for the 70-day specimens, epithelial pearls are present in the midline of the hard palate. Thus soft palate fusion is complete between 70 and 74-days.

3.2.5 3-D reconstructions confirm an epithelial seam is present in the soft palate

In order to clarify the relationship of a seam to the soft and hard palate I reconstructed a variety of specimens ranging in age from 54 to 74-days (54-days n = 2, 57-days n = 4, 59 days n = 2, 64-days n = 1, 67-days n = 1, 70-days n = 1, 74-days n = 1). I traced outlines for the palatal shelves of the hard and soft palate, the nasal septum, the palatine process of the maxilla and palatine bones, the greater palatine nerve, and the midline seam, and seam remnants when present. In the 54-day specimen, a midline seam is present in the entire soft palate ending where the palate has not yet fused (Fig 3.6A,B). In the posterior aspect of the unfused soft palate, the shelves are diminutive in length and have a rounder, mushroom shape than the actively fusing parts of the shelf. These dome-shaped shelves appear tethered to the lateral pharyngeal wall, and will have to reorient and grow outwards towards the midline before these soft palate shelves can touch in the midline. A midline epithelial seam was also present throughout the hard palate and into the soft palate in the 57-day specimens traced (Fig 3.6C,D and data not shown H9517, H10142, H10458). The terminal portions of the soft palate shelves in these 57 day specimens start to take on a different shape, they have lost the dome-like shape projecting from the pharyngeal walls and become more thin and tapered as they elongate toward the midline. By the 64th day, the medial epithelial seam (Fig 3.6E,F) has degraded. I also traced the outline of the aponeurosis because the condensations were clearly visible in the 64-day specimen. In the 70-day specimen, the shape of the soft palate

has changed as the uvula is developing (Fig 3.6G, H9832). There is an abrupt change from a horizontal to vertical orientation of the soft palate of this 70-day specimen at the posterior aspect and a midline seam can be seen only in the developing uvula (Fig 3.6G, H9832). By 74-days (data not shown, H9819), the hard and soft palate morphology is fully formed, including the uvula. There is a continuous aponeurosis across the soft palate. No seam remains, however a few epithelial pearls are present in the midline of the hard palate (data not shown, H9819).

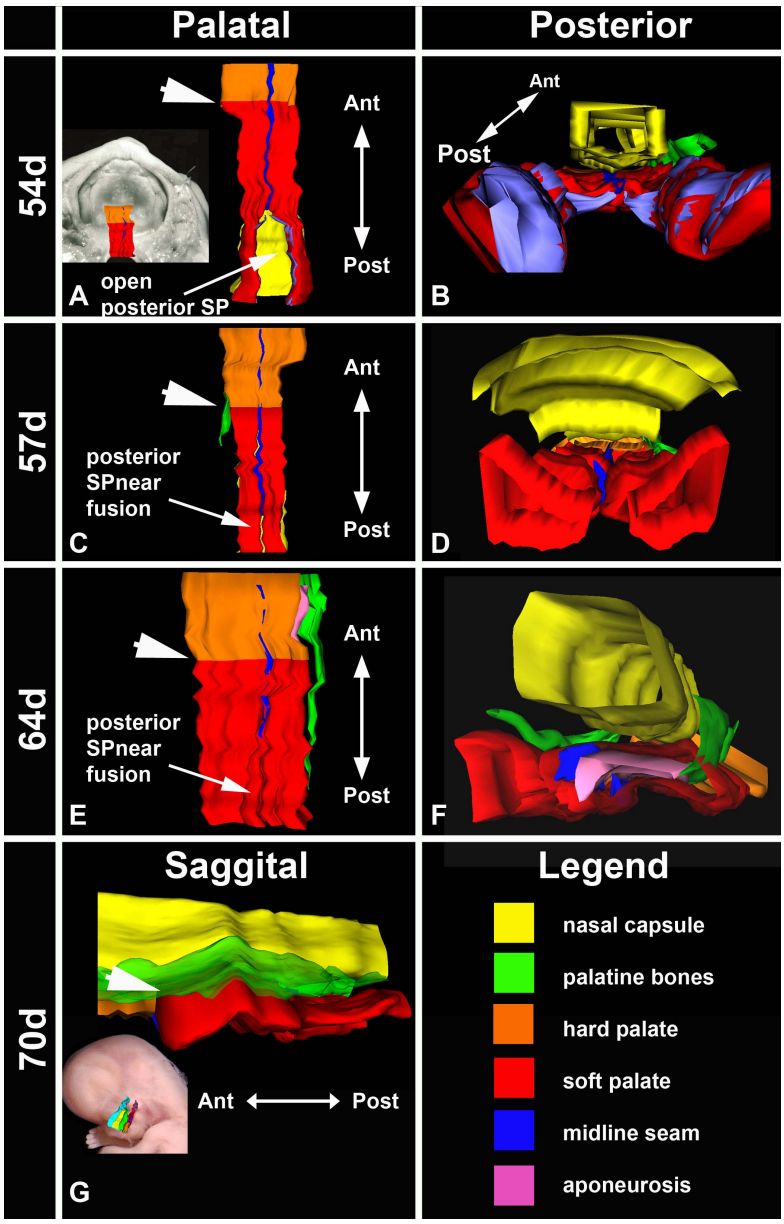

Figure 3.6. 3D reconstructions of the hard palate-soft palate junction

All specimens are shown from a palatal and a posterior view, with the exception of the 70-day specimen (G), which is displayed from a sagittal view. White arrowheads point to the hard palate-soft palate junction . In the 54-day specimen (A, B), the seam is present through the entire fused soft palate (red). The unfused soft palate shelves in this reconstruction are significantly smaller in volume than the fused shelves, indicating that they may need to increase in volume before they can contact and fuse. This is also demonstrated from the posterior view (B), where the dome shape of these unfused shelves can be clearly seen. In the 57-day specimen (C, D), the midline seam is proliferating through the entire fused hard and soft palate (blue). The unfused shelves in this specimen are larger in volume and closer to contacting in the midline(C, D) than the shelves of the 54-day specimen (A, B).). The 57 day shelves also have a different shape, they are more tapered in appearance. In the 64-day specimen (E, F), the seam in the hard palate and initial soft palate is still present (blue), then in the anterior soft palate it has disappeared, then reappears in the middle to posterior fusing soft palate. The aponeurosis (purple) can also be seen migrating in to the left palatal shelf (F). In the sagittal reconstruction of the 70-day specimen (G) we can see the change in location of the soft palate (red) from the hard palate (orange) as the soft palate hangs lower than the hard palate, representing the transition from a horizontal to a more vertically-oriented structure.

3.2.6 Palatine aponeurosis condenses near the tensor veli palatini between 59 and 67d

By 59 days, the majority of the muscles of the fetal craniofacial complex have begun to develop. In the 59 day specimen stained with MF20 antibody (Fig 3.7A,B,C), the tongue muscle is prominent and the medial pterygoid and the masseter muscle can be seen lying on either side of Meckel's cartilage (Fig 3.7A). At a more posterior location in the 59 day specimen (Fig 3.7B), the tensor veli palatini muscle can be clearly seen in its position lateral to the developing pterygoid hamulus, the levator veli palatini is developing within the body of the soft palate and early signs of the palatoglossus muscle can be seen sitting more inferiorly at the base of the tongue. The palatopharyngeus can also be seen in its early stage of development (Fig 3.7C). By 67-days (Fig. 3.7 D,D',E,E',F,F') the muscles are more robust and organized. The condensation of the developing aponeurosis can be seen (Fig 3.7D,E insets). The palatoglossus is migrating superiorly towards the soft palate (Fig 3.7E) and the palatopharyngeus is increasing in mass (Fig 3.7F, F'). By day 74 (data not shown, H9819), the aponeurosis has migrated across the soft palate and has attached to the tensor veli palatini to develop its postnatal morphology.

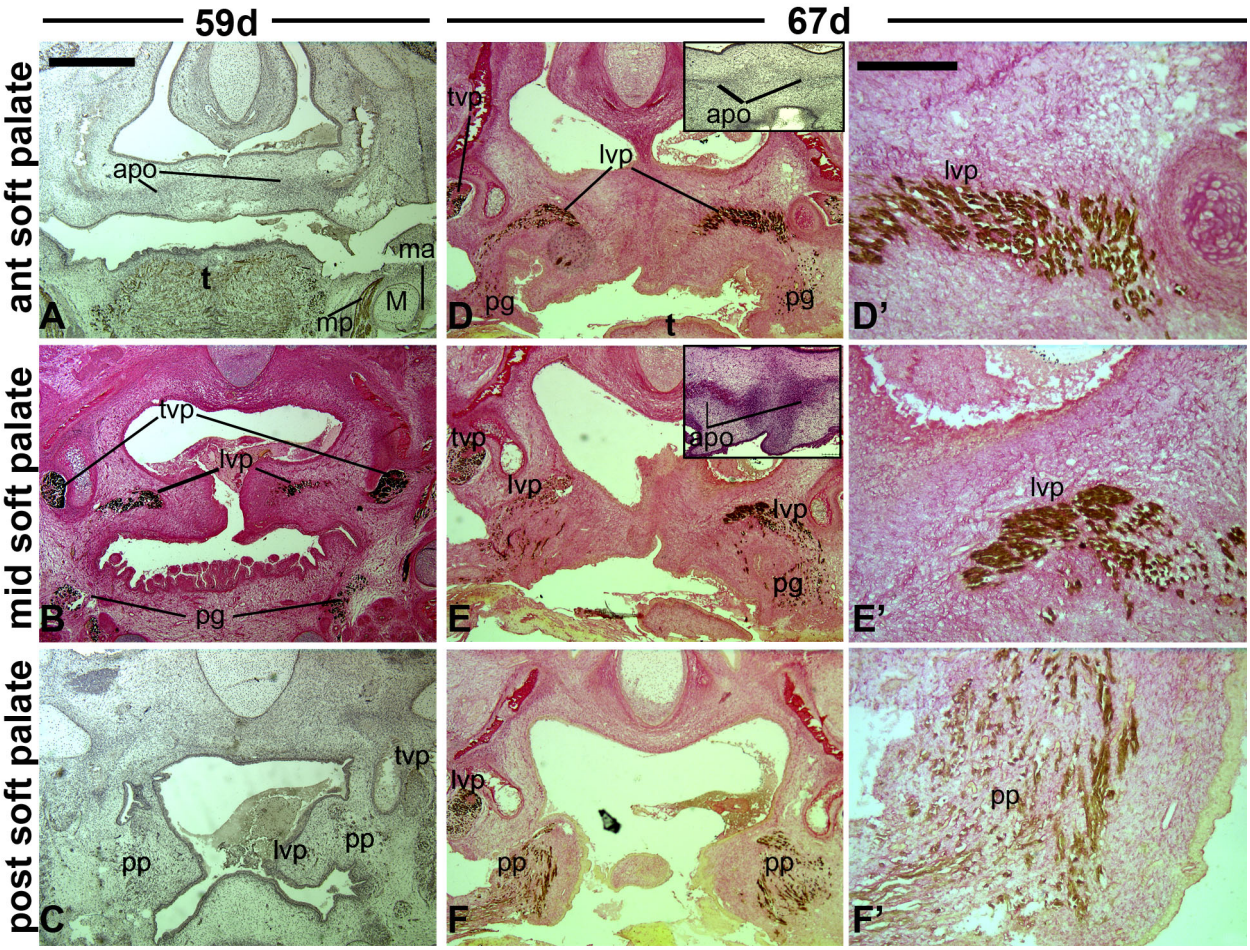

Figure 3.7. Palatal muscle development in 59 and 67-day fetuses.

Frontal sections of 59 and 67-day specimens through the soft palate. Muscle cells stained with MF20 antibody. Specimens counterstained with either hematoxylin and eosin (A, C) or Picrosirius Red and Alcian Blue. In the 59 day specimen (A-C), many muscles can be seen developing. In the anterior soft palate (A), the aponeurosis is seen in the palatal shelves, the tongue muscle is evident and the medial pterygoid and masseter muscles are visible developing on the medial and lateral aspects respectively of the developing mandible and Meckels cartilage. In the middle of the soft palate (B), the shelves have not yet fused. The tvp is visible on the lateral side of the pterygoid hamulus and the lvp is developing in the middle of the palatal shelves. The palatoglossus muscles are also visible. In the posterior soft palate (C), the palatopharyngeus muscle cells are starting to form. In the 67-day specimen, the lvp muscle is more defined in the anterior and middle soft palate (D, D', E, E'). The palatine aponeurosis is thicker and more condensed and is almost continuous across the middle of the palate (D, E insets). The palatopharyngeus muscle is becoming larger and more organized (F, F') than in the 59 day specimen (C). Key: Key: apo – palatine aponeurosis, lvp – levator veli palatini, ma – masseter, M – Meckels cartilage, mp - medial pterygoid, pg – palatoglossus, pp- palatopharyngeus, tvp – tensor veli palatini, t – tongue, scale bar in A =525μm, applies to A,B,C,D,E,F; scale bar in D' =200μm, applies to D',E',F'.

Chapter 4 –Discussion

4.1. Revised model of soft palate development

The results of my study have shown that fusion of the palatal shelves is the main mechanism by which the soft palate forms. As palatal shelf fusion occurs in an anterior to posterior direction, the soft palate shelves grow out from the lateral wall of the pharynx towards the midline and contact to form a midline epithelial seam (Fig 4.1A-C). My study advocates that the process of fusion is occurring throughout the soft palate into the uvula, as one 70-day specimen (H9705) showed the presence of a midline epithelial seam extending into the tip of the uvula. This contradicts the theory proposed by Burdi and Faist (Burdi and Faist, 1967), but clear cut evidence of a midline seam in the soft palate supports fusion as the prevailing method of soft palate development.

The unanticipated finding in my study was that are independent rates of development being followed in the hard and soft palate. The hard palate seam fusion progresses rather slowly from anterior to posterior. Thus I often encountered robust seams in the posterior hard palate. Yet the soft palate seam forms and degrades very rapidly. Thus there are specimens in which the anterior soft palate seam is degrading or completely removed at the same time when the posterior hard palate seam is largely intact. This is best seen in the 64 day specimen (Fig. 3.5). The hard palate seam can persist from the time of fusion to birth, a 34 week time period. The soft palate seam was only seen for a 16 day time period, from 54-70 days. It will be important to expand my sample to confirm this novel idea.

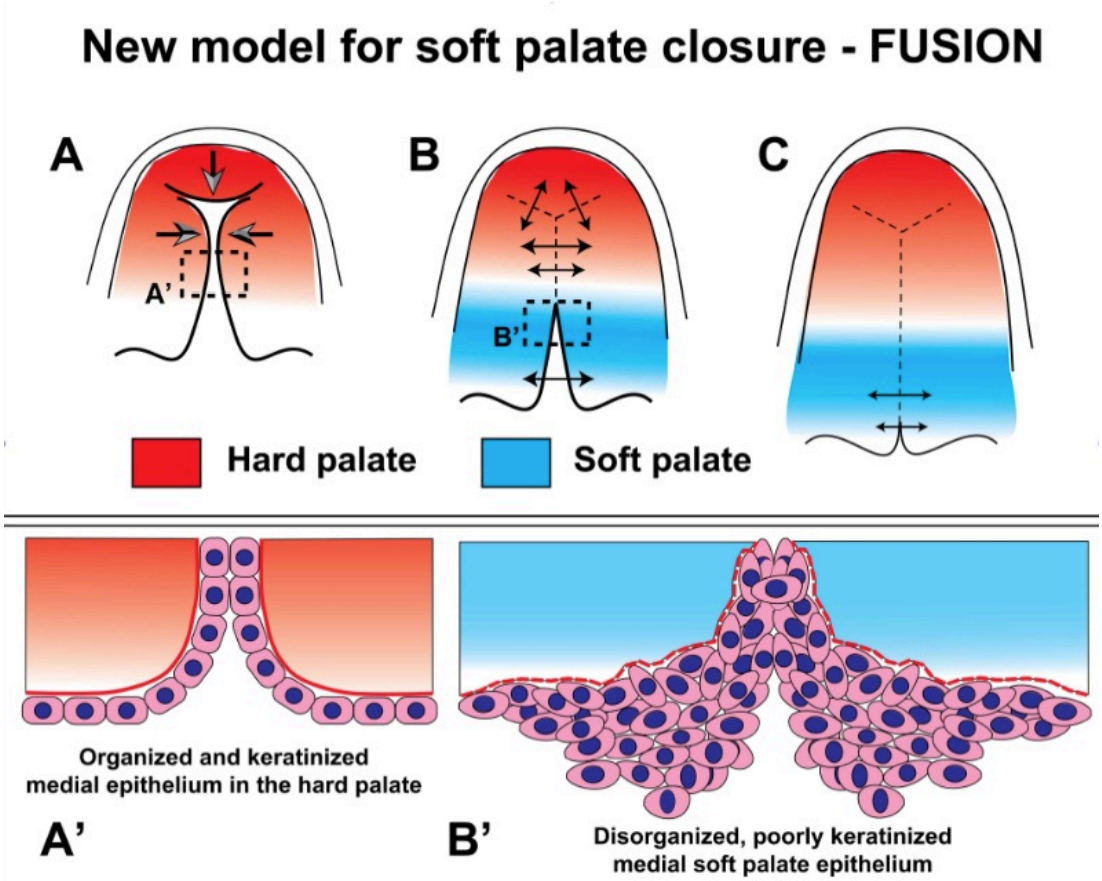

Figure 4.1. The mechanism of palate closure is fusion in both the hard and soft palate.

This diagrammatic representation is an update of the diagram included in the 1967 study on palatal morphogenesis by Burdi and Faist. It illustrates my proposed method of soft palate development. Hard palate development is unchanged from the previous diagram with outgrowth of the palatal shelves towards the midline and primary palate. The gradients indicate the maturity of the seam. The darker the colour the more mature. There is a disconnect between the rate of maturation of the seam in the hard and soft palates such that the two structures appear to be forming almost independently of each other. The soft palate seam may be completely removed at the same time as there is a seam present in the posterior hard palate. (A), contact occurs and the shelves fuse in an anterior-posterior direction (B,). As the hard palate is fusing, the soft palate shelves are growing outwards from the lateral pharyngeal wall and contacting in the midline (B), after which point fusion occurs and the midline epithelial seam is degraded (C). The inserts show the differences in the appearance of the hard vs soft palate epithelium at the point of fusion. The hard palate epithelium (A') is highly organized, displays an intact basement membrane and is keratinized, based on the contrast in epithelial and mesenchymal cell staining. The soft palate epithelium (B') is disorganized and bulky, with clumping of cells and a fragmented basement membrane. There is also poor keratinization of the soft palate epithelial cells.

It is important to note the differences in the appearance of the epithelium between the hard and soft palate during fusion (Fig 4.1A', B'). The epithelium of the hard palate is regular and uniform in appearance. It is approximately 2-3 cells thick, stains darkly with H&E compared to the mesenchymal cells, and has distinct staining compared to the mesenchyme which suggests an intact basement membrane. Conversely the soft palate epithelium is very disorganized in appearance. It is much bulkier and less regular in appearance than the hard palate, ranging from 2-20 cells thick. With both H&E and Picrosirius Red staining, the epithelial cells only stain very lightly and are difficult to distinguish from the mesenchyme, due to poor keratinization of the soft palate epithelium. The basement membrane in the soft palate may be fragmented and difficult to identify. Future studies should examine more closely the different types of keratins in hard and soft palate seam as well as the presence of basement membrane.

These differences are likely due to the different embryonic origins of the two structures. While no direct evidence exists from experimental studies, some anatomists have postulated that the hard palate epithelium arises from ectoderm from the stomodeum, whereas the soft palate originates from foregut endoderm (Singh, 2005). In a study on the regulation of Shh in mice found there was an enhancer that drove expression in the soft palate and pharyngeal epithelium. When this enhancer was deleted the soft palate was shortened, the epiglottis and posterior tongue were abnormal. It was not possible to separate out the regulation of gene expression in the soft palate from that of the pharynx which supports a common embryonic origin (Sagai et al., 2009). These different origins may also be responsible for the temporal differences in seam degradation between the hard and soft palates.

4.2. Comparative Anatomy - Do other mammals have a seam in the soft palate?

In this section I will provide a broader perspective on how representative human soft palate fusion is in relation to other mammals. During evolution of mammals the assumption is that developmental mechanisms would be conserved. Certainly it is true that all mammals pass through a stage of palatal shelf morphogenesis, reorientation and fusion but whether or not a seam is present in the soft palate has not received as much attention. In the mouse it is well known that the soft palate in mice develops by fusion, not merging (Smiley, 1975) . Ultrastructural studies were performed on hamster palates (Shah and Chaudhry, 1974). Palatal closure occurred in hamsters between days 12 and 13 of gestation, with soft palate closure occurring over a four hour time period during these days. Prior to fusion, the medial edge epithelia of the shelves appeared thickened. Fusion was seen between soft palate shelves via desmosomal attachments, creating a midline epithelial seam with basal lamina on either side. Removal of the seam was observed by apoptosis, exfoliation and migration of epithelial cells (Shah and Chaudhry, 1974).

Rather surprisingly, no rat studies have looked at an exact mechanism of soft palate development, however it has been shown that there is a higher rate of epithelial cell renewal in the soft palate of rats versus the hard palate, which may indicate why a midline epithelial seam would break down faster in the soft palate than the hard palate (Hayward, 1973; Hayward et al., 1973).

There is a single study performed on non-human primates. In this study 37 baboon embryos were analyzed between 30 and 64-days (estimated) post conception (Bollert and Hendrickx, 1971). In the 53 day and older specimens, the soft palates were formed with the exception of the uvula, which was still not formed in the oldest 64-day specimens. Upon inspection of these specimens, no epithelial remnants were seen in the soft palate, so the authors concluded that the soft palate must form by merging, however this may not actually be the mechanism of baboon soft palate development. Taken together, the evidence from mouse and hamster suggests that the most likely mechanism of soft palate closure in mammals is fusion. In other words it is hard to imagine that a different mechanism of palatogenesis of the soft palate would evolve in primates and humans.

4.3. Variability of palate development in human fetuses

In my study, there was a degree of variability seen amongst the specimens, in particular two precocious specimens at 54 and 59 days had palates developed beyond those of older specimens (Table 3.1, 3.2). There are many different factors that could contribute to the variability. Variations in form and development are intrinsic to all humans. Only in monozygotic twins would we be able to eliminate the genetic variability of development. Maternal factors also play a role in palatogenesis. Maternal smoking and amount of folic acid intake have both been shown to contribute to orofacial clefting in children (Butali et al., 2013). Certain medications such as cortisone and phenytoin also increase clefting rates (Carinci et al., 2007). Low amniotic fluid levels alter the

environment in which an embryo is developing. Sex differences and racial variations also exist in embryo size and timing of development (O'Rahilly and Muller, 2010). Males tend to have secondary palates that orient from vertical to horizontal earlier than females (Burdi and Silvey 1969), and the sex was not reported for any of the specimens collected in my study. Palate development takes place over a period of weeks (from weeks 6-12 postconception), thus it is normal to expect some degree of variation in different specimens. There was a 16 day window in my specimens in which a seam was visible: from days 54-70. Thus specimens observed have to be old enough that the soft palate shelves are in contact (ie 54 days and older), but young enough that the aponeurosis is not fully formed. In the 70 day specimen the only remaining soft palate seam was at the apex of the uvula.

Despite the intrinsic variability in development, is important to make every effort to be as accurate and rigorous as possible when dating the age of the human specimens. The criteria utilized at the University of Washington, where the tissue for this study was obtained, includes estimations from prenatal intakes, and the external measurements: foot length, Streeter's stage and crown-rump length. Burdi and Faist only used crown-rump length and age in weeks to determine fetal age. The more factors utilized, the more accurate age dating of a specimen can be, however the information obtained from the University of Washington allowed me to directly compare the crown-rump lengths of my specimens with those of Burdi and Faist (Table 3.3). The increased range of crown rump lengths during development of the soft palate allowed me to see midline epithelial seams in the soft palate from the anterior aspect all the way to the uvula during various stages of development.

Overall, the specimens analyzed by Burdi and Faist followed the same general developmental milestones as my specimens, with some variability as well. Their specimens had initial secondary palate closure between 29 and 37mm crown-rump length. Complete soft palate closure was only seen in Burdi and Faist's oldest specimen, measuring 75mm crown-rump length. My oldest specimen was also 75mm, and was also the only specimen in my collection that exhibited complete palatogenesis of the hard and soft palate.

4.4. Animal models give insights into the genes that are required for soft palate morphogenesis

There are hundreds of mouse models with cleft secondary palate but only a handful have a true submucous cleft. The Osr2-IresCre; *Bmpr1a* $^{fl/fl}$ (Bone Morphogenetic Protein Receptor 1a) (Baek et al., 2011) mouse is a mutant which displays inactivation of *Bmpr1a* in the palatal mesenchyme, resulting in a submucous cleft of the anterior soft palate. The phenotype of this mutant also included a gap between the primary and secondary palate and an irregular appearance of the palatal rugae. There was a lack of condensation of mesenchyme and agenesis of the palatine process of the maxilla. The palatal process of the palatine bone also has a decrease in osteogenesis and was diminutive in size. *Bmpr1a* mRNA is expressed in the mesenchyme of the medial nasal prominences and in the anterior half of the palatal shelves, with very little expression in posterior secondary palate. This mouse model indicates that *Bmpr1a* is required in the palatal

mesenchyme for normal palatogenesis and palatal bone development to occur. This submucous cleft phenotype of the Osr2-IresCre; Bmpr1a $^{fl/fl}$ mouse arose from the combination of significantly reduced proliferation of the palatal mesenchymal and a lack of palatal bone support in the developing fetus.

A signal that is directly involved in epithelial fusion of the palate is the protein, Transforming growth factor beta 3 (Tgf-β3). Tgf-β3 null mouse mutants (*Tgf-β3*-/-) all exhibit some degree of clefting of the palate (Kaartinen et al., 1997; Kaartinen et al., 1995; Proetzel et al., 1995). The C57BL/6 background exhibits the most severe clefting phenotype with 50% of the mutants having complete clefts and the other 50% having partial clefts (Cui et al., 2005). Tgf-β3 regulates the disappearance of the medial edge epithelium in palatal shelf fusion, and knocking out this gene has a profound effect on shelf fusion. Tgf-β3 directly regulates the phosphorylation of the transcription factor, Smad2, so when Smad2 was overexpressed in the medial edge epithelium on a transgene, the cleft palate phenotype was rescued in Tgf-β3-/-(Cui et al., 2005). Of the 6 null mutant mice who carried the K14-Smad2 transgene (Tgf-β3-/-/K14-Smad2), none had complete clefts, and 3 had fusion into the soft palate. In the 5 Tgf-β3-/-, 4 had complete clefts and only one had partial clefting (Cui et al., 2005).

A study in which the receptor, *Tgfbr2* was conditionally deleted in the epithelium also generated submucous clefts in 100% of the offspring as well as cleft soft palate (Xu et al., 2006). Here the mechanism underlying the submucous cleft phenotype included excessive cell proliferation and lack of apoptosis. This allowed the midline epithelial seam to persist instead of degrade. Interestingly, the

expression of the transcription factor Irf6 was lacking in the epithelium. Mutations in the gene *IRF6* cause Van der Woude's Syndrome (Kondo et al., 2002). Thus decreased IRF6 levels could be contributing to non-syndromic submucous clefts or other microforms of cleft palate. Recently *TGFBR1* and *TGBR2* mutations have been shown to cause Loeys-Dietz syndrome (Breckpot et al., 2010; Cardoso et al., 2012; Loeys et al., 2005; Loeys and Dietz, 1993; Singh et al., 2006). A striking feature of the syndrome is bivid uvula and/or cleft palate. This is all the more reason to investigate the expression of the receptors for TGFβ in the soft palate.

Downstream of TGFβ signaling is the transcription factor *Smad4*. In conditional mouse knockouts of *Smad4* in the ectoderm there is no palate phenotype. However when these mice are crossed to the mice heterozygous for a loss-of-function mutation in *Irf6*, 100% of the embryos have submucous clefts (Iwata et al., 2013). This is possibly the most penetrant cleft affecting the soft palate that has been reported in a mouse model.

In the *Tbx22* knockout mouse mutant (Tbx22-/-)(Pauws et al., 2009a) fetuses exhibited a translucent area in the posterior palate. There was severely reduced bone formation in the posterior palate, despite the fact that the palatal shelves had fully fused. Some mutants even exhibited complete cleft palate, whereas others displayed submucous cleft palate with reduced bone formation and delayed osteoblast differentiation. As mentioned previously human mutations in *TBX22* cause X-linked ankyloglossia and cleft palate which further supports a role for *TBX22* in soft palate morphogenesis.

Another member of the T-box family, Tbx1, is also considered to be a major candidate gene for the pathogenesis of 22q11.2 deletion syndrome in humans (also known as DiGeorge syndrome or velo-cardio-facial syndrome). DiGeorge or 22q11.2 deletion syndrome (OMIM #188400) has an incidence of approximately 1/4000 live human births and commonly the patients will exhibit complete cleft palate or submucous cleft and velopharyngeal insufficiency (Scambler, 2000). In the Tbx1-/- mouse mutant (Funato et al., 2012), all of the null mutants displayed an array of palatal deformities including compete clefts (41%), anterior clefts and an incomplete cleft palate (47%), and anterior clefts and soft palate clefts (12%). None of the wild type or Tbx1+/- haploinsufficient mutants had any form of clefting. Whole mount staining showed high expression of Tbx1 in the medial edge epithelium of the palatal shelves prior to fusion suggesting that this transcription factor is mediating signaling during epithelial adhesion and fusion.

4.5 Limitations of this study

Due to the length of time the human specimens in my study spent in storage media, it was difficult to get any useable results from molecular tests. Pilot tests were performed using TUNEL assays and PCNA (Proliferating Nuclear Cell Antigen), however no information was obtained. Future directions for this project will involve performing TUNEL and PCNA on recently collected specimens that were tested for RNA viability and stored in 70% EtOH. TUNEL will show if apoptosis is taking place

in the midline of the soft palate to degrade the midline epithelial seam. PCNA or another cell cycle antibody would indicate the pattern of cell proliferation in the developing soft palate.

Based on the work of the previously discussed mouse models of submucous clefting, there are a number of candidate genes that would be valuable to create probes for to use in radioactive in-situ hybridizations. These include *BMPR1A*, *TGFBR2*, *TBX22, TGFB3, IRF6 and TBX1.*

Another limitation of my study was that it was sometimes difficult to differentiate the epithelium from the mesenchyme in the soft palate. Thus I was not able to reliably score the presence of epithelial islands in all of the sections. In future work it would be advantageous to use a pan-cytokeratin antibody which works well to detect epithelium in a wide variety of species. I believe this antibody would be robust enough to work on previously collected human samples.

The Winsurf 3D reconstruction program could have been used to measure area of each segmented region and then when combined with spacing between sections it would have been possible to calculate volume changes during development. These quantitative data would have provided additional insights into the dramatic growth of the soft palate.

Finally I would like to increase the number of samples in my study and to investigate human fetuses from other populations. This would add more weight to my study since it would show that fusion is a widespread phenomenon that is not restricted to European ethnicity. It would also allow me to utilize a statistical power

analysis to determine mathematically if my hypothesis is true. It would involve grouping specimens of the same or similar ages to create multiple groups which could be used to compare seam development at different timepoints, and gain more definitive results of what a soft palate seam should look like at a given age (eg 54-57 days, 59-64 days, 67-70 days and 74+days). One possible test to use would be the Chi-squared distribution to compare groups and validate my hypothesis.

References

Abbott, B. D., 2010. The etiology of cleft palate: a 50-year search for mechanistic and molecular understanding. Birth defects research. Part B, Developmental and reproductive toxicology. 89**,** 266-74.

Altman, D. G., Chitty, L. S., 1997. New charts for ultrasound dating of pregnancy. Ultrasound in obstetrics & gynecology : the official journal of the International Society of Ultrasound in Obstetrics and Gynecology. 10**,** 174-91.

Baek, J. A., Lan, Y., Liu, H., Maltby, K. M., Mishina, Y., Jiang, R., 2011. Bmpr1a signaling plays critical roles in palatal shelf growth and palatal bone formation. Dev Biol. 350**,** 520-31.

Beaty, T. H., Murray, J. C., Marazita, M. L., Munger, R. G., Ruczinski, I., Hetmanski, J. B., Liang, K. Y., Wu, T., Murray, T., Fallin, M. D., Redett, R. A., Raymond, G., Schwender, H., Jin, S. C., Cooper, M. E., Dunnwald, M., Mansilla, M. A., Leslie, E., Bullard, S., Lidral, A. C., Moreno, L. M., Menezes, R., Vieira, A. R., Petrin, A., Wilcox, A. J., Lie, R. T., Jabs, E. W., Wu-Chou, Y. H., Chen, P. K., Wang, H., Ye, X., Huang, S., Yeow, V., Chong, S. S., Jee, S. H., Shi, B., Christensen, K., Melbye, M., Doheny, K. F., Pugh, E. W., Ling, H., Castilla, E. E., Czeizel, A. E., Ma, L., Field, L. L., Brody, L., Pangilinan, F., Mills, J. L., Molloy, A. M., Kirke, P. N., Scott, J. M., Arcos-Burgos, M., Scott, A. F., 2010. A genome-wide association study of cleft lip with and without cleft palate identifies risk variants near MAFB and ABCA4. Nat Genet. 42**,** 525-9.

Beaty, T. H., Ruczinski, I., Murray, J. C., Marazita, M. L., Munger, R. G., Hetmanski, J. B., Murray, T., Redett, R. J., Fallin, M. D., Liang, K. Y., Wu, T., Patel, P. J., Jin, S. C., Zhang, T. X., Schwender, H., Wu-Chou, Y. H., Chen, P. K., Chong, S. S., Cheah, F., Yeow, V., Ye, X., Wang, H., Huang, S., Jabs, E. W., Shi, B., Wilcox, A. J., Lie, R. T., Jee, S. H., Christensen, K., Doheny, K. F., Pugh, E. W., Ling, H., Scott, A. F., 2011. Evidence for gene-environment interaction in a genome wide study of nonsyndromic cleft palate. Genet Epidemiol. 35**,** 469-78.

Beaty, T. H., Taub, M. A., Scott, A. F., Murray, J. C., Marazita, M. L., Schwender, H., Parker, M. M., Hetmanski, J. B., Balakrishnan, P., Mansilla, M. A., Mangold, E., Ludwig, K. U., Noethen, M. M., Rubini, M., Elcioglu, N., Ruczinski, I., 2013. Confirming genes influencing risk to cleft lip with/without cleft palate in a case-parent trio study. Hum Genet.

Bell, J. C., Raynes-Greenow, C., Bower, C., Turner, R. M., Roberts, C. L., Nassar, N., 2013. Descriptive epidemiology of cleft lip and cleft palate in Western Australia. Birth defects research. Part A, Clinical and molecular teratology. 97**,** 101-8.

Birnbaum, S., Ludwig, K. U., Reutter, H., Herms, S., Steffens, M., Rubini, M., Baluardo, C., Ferrian, M., Almeida de Assis, N., Alblas, M. A., Barth, S., Freudenberg, J., Lauster, C., Schmidt, G., Scheer, M., Braumann, B., Berge, S. J., Reich, R. H., Schiefke, F., Hemprich, A., Potzsch, S., Steegers-Theunissen, R. P., Potzsch, B., Moebus, S., Horsthemke, B., Kramer, F. J., Wienker, T. F., Mossey, P. A., Propping, P., Cichon, S.,

Hoffmann, P., Knapp, M., Nothen, M. M., Mangold, E., 2009. Key susceptibility locus for nonsyndromic cleft lip with or without cleft palate on chromosome 8q24. Nat Genet. 41**,** 473-7.

Bollert, J. A., Hendrickx, A. G., 1971. Morphogenesis of the palate in the baboon (Papio cynocephalus). Teratology. 4**,** 343-54.

Braybrook, C., Doudney, K., Marcano, A. C., Arnason, A., Bjornsson, A., Patton, M. A., Goodfellow, P. J., Moore, G. E., Stanier, P., 2001. The T-box transcription factor gene TBX22 is mutated in X-linked cleft palate and ankyloglossia. Nat Genet. 29**,** 179-83.

Breckpot, J., Budts, W., De Zegher, F., Vermeesch, J. R., Devriendt, K., 2010. Duplication of the TGFBR1 gene causes features of Loeys-Dietz syndrome. Eur J Med Genet. 53**,** 408-10.

Burdi, A., Faist, K., 1967. Morphogenesis of the Palate in Normal Human Embryos with Special Emphasis on the Mechanisms Involved. American Journal of Anatomy. 120**,** 149-160.

Bush, J. O., Jiang, R., 2012. Palatogenesis: morphogenetic and molecular mechanisms of secondary palate development. Development. 139**,** 231-43.

Butali, A., Little, J., Chevrier, C., Cordier, S., Steegers-Theunissen, R., Jugessur, A., Oladugba, B., Mossey, P. A., 2013. Folic acid supplementation use and the MTHFR C677T polymorphism in orofacial clefts etiology: An individual participant data pooled-analysis. Birth defects research. Part A, Clinical and molecular teratology.

Cardoso, S., Robertson, S. P., Daniel, P. B., 2012. TGFBR1 mutations associated with Loeys-Dietz syndrome are inactivating. J Recept Signal Transduct Res. 32**,** 150-5.

Carinci, F., Scapoli, L., Palmieri, A., Zollino, I., Pezzetti, F., 2007. Human genetic factors in nonsyndromic cleft lip and palate: an update. Int J Pediatr Otorhinolaryngol. 71**,** 1509-19.

Cohen, S. R., Chen, L., Trotman, C. A., Burdi, A. R., 1993. Soft-palate myogenesis: a developmental field paradigm. The Cleft palate-craniofacial journal : official publication of the American Cleft Palate-Craniofacial Association. 30**,** 441-6.

Cohlan, S. Q., 1953. Excessive intake of vitamin A as a cause of congenital anomalies in the rat. Science. 117**,** 535-6.

Cuervo, R., Covarrubias, L., 2004. Death is the major fate of medial edge epithelial cells and the cause of basal lamina degradation during palatogenesis. Development. 131**,** 15-24.

Cuervo, R., Valencia, C., Chandraratna, R. A., Covarrubias, L., 2002. Programmed cell death is required for palate shelf fusion and is regulated by retinoic acid. Dev Biol. 245**,** 145-56.

Cui, X. M., Chai, Y., Chen, J., Yamamoto, T., Ito, Y., Bringas, P., Shuler, C. F., 2003. TGF-beta3-dependent SMAD2 phosphorylation and inhibition of MEE proliferation during palatal fusion. Dev Dyn. 227**,** 387-94.

Cui, X. M., Shiomi, N., Chen, J., Saito, T., Yamamoto, T., Ito, Y., Bringas, P., Chai, Y., Shuler, C. F., 2005. Overexpression of Smad2 in Tgf-beta3-null mutant mice rescues cleft palate. Dev Biol. 278**,** 193-202.

De la Cuadra Blanco, C., Peces Pena, M. D., Rodriguez-Vazquez, J. F., Merida-Velasco, J. A., Merida-Velasco, J. R., 2012. Development of the human tensor veli palatini: specimens measuring 13.6-137 mm greatest length; weeks 6-16 of development. Cells Tissues Organs. 195**,** 392-9.

Diewert, V. M., 1981. Correlation between alterations in Meckel's cartilage and induction of cleft palate with beta-aminoproprionitrile in the rat. Teratology. 24**,** 43-52.

Diewert, V. M., 1985. Development of human craniofacial morphology during the late embryonic and early fetal periods. American journal of orthodontics. 88**,** 64-76.

Diewert, V. M., 1986. Craniofacial growth during human secondary palate formation and potential relevance of experimental cleft palate observations. Journal of craniofacial genetics and developmental biology. Supplement. 2**,** 267-76.

Diewert, V. M., Pratt, R. M., 1981. Cortisone-induced cleft palate in A/J mice: failure of palatal shelf contact. Teratology. 24**,** 149-62.

Dixon, M. J., Marazita, M. L., Beaty, T. H., Murray, J. C., 2011. Cleft lip and palate: understanding genetic and environmental influences. Nat Rev Genet. 12**,** 167-78.

Dudas, M., Nagy, A., Laping, N. J., Moustakas, A., Kaartinen, V., 2004. Tgf-beta3-induced palatal fusion is mediated by Alk-5/Smad pathway. Dev Biol. 266**,** 96-108.

Fitchett, J. E., Hay, E. D., 1989. Medial edge epithelium transforms to mesenchyme after embryonic palatal shelves fuse. Dev Biol. 131**,** 455-74.

Fraser, F. C., Fainstat, T. D., 1951. Production of congenital defects in the off-spring of pregnant mice treated with cortisone; progress report. Pediatrics. 8**,** 527-33.

Fraser, F. C., Kalter, H., Walker, B. E., Fainstat, T. D., 1954. The experimental production of cleft palate with cortisone and other hormones. Journal of cellular physiology. Supplement. 43**,** 237-59.

Funato, N., Nakamura, M., Richardson, J. A., Srivastava, D., Yanagisawa, H., 2012. Tbx1 regulates oral epithelial adhesion and palatal development. Hum Mol Genet. 21**,** 2524-37.

Garcia Velasco, M., Ysunza, A., Hernandez, X., Marquez, C., 1988. Diagnosis and treatment of submucous cleft palate: a review of 108 cases. The Cleft palate journal. 25**,** 171-3.

Gilbert, P. W., 1952. The Origin of the Human Extrinsic Ocular Muscles. Anatomical Record. 112**,** 333-334.

Grant, S. F., Wang, K., Zhang, H., Glaberson, W., Annaiah, K., Kim, C. E., Bradfield, J. P., Glessner, J. T., Thomas, K. A., Garris, M., Frackelton, E. C., Otieno, F. G., Chiavacci, R. M., Nah, H. D., Kirschner, R. E., Hakonarson, H., 2009. A genome-wide association study identifies a locus for nonsyndromic cleft lip with or without cleft palate on 8q24. The Journal of pediatrics. 155**,** 909-13.

Greene, R. M., Pisano, M. M., 2010. Palate morphogenesis: current understanding and future directions. Birth defects research. Part C, Embryo today : reviews. 90**,** 133-54.

Gritli-Linde, A., 2007. Molecular control of secondary palate development. Dev Biol. 301**,** 309-26.

Ha, K. M., Cleland, H., Greensmith, A., Chong, D., Macgill, K., Verhoeven, A., Hutson, J. M., 2013. Submucous cleft palate: an often-missed diagnosis. The Journal of craniofacial surgery. 24**,** 878-85.

Hadlock, F. P., Deter, R. L., Carpenter, R. J., Park, S. K., 1981. Estimating fetal age: effect of head shape on BPD. AJR. American journal of roentgenology. 137**,** 83-5.

Hayward, A. F., 1973. Electron microscopic observations on cell coat and membrane-coating granules of the epithelium of the hard and soft palate in the rat. Arch Oral Biol. 18**,** 67-75.

Hayward, A. F., Hamilton, A. I., Hackemann, M. M., 1973. Histological and ultrastructural observations on the keratinizing epithelia of the palate of the rat. Arch Oral Biol. 18**,** 1041-57.

Hern, W. M., 1984. Correlation of fetal age and measurements between 10 and 26 weeks of gestation. Obstetrics and gynecology. 63**,** 26-32.

Itani, O., Prophit, C., May, D., Shekhawat, P., 2000. Special feature: radiological case of the month. Velopharyngeal insufficiency causing nasopharyngeal reflux in the neonate. Archives of pediatrics & adolescent medicine. 154**,** 1167-8.

Iwata, J., Suzuki, A., Pelikan, R. C., Ho, T. V., Sanchez-Lara, P. A., Urata, M., Dixon, M. J., Chai, Y., 2013. Smad4-Irf6 genetic interaction and TGFbeta-mediated IRF6 signaling cascade are crucial for palatal fusion in mice. Development. 140**,** 1220-30.

Jiang, R., Bush, J. O., Lidral, A. C., 2006. Development of the upper lip: morphogenetic and molecular mechanisms. Dev Dyn. 235**,** 1152-66.

Jin, J. Z., Ding, J., 2006. Analysis of cell migration, transdifferentiation and apoptosis during mouse secondary palate fusion. Development. 133**,** 3341-7.

Jussila, M., Thesleff, I., 2012. Signaling networks regulating tooth organogenesis and regeneration, and the specification of dental mesenchymal and epithelial cell lineages. Cold Spring Harb Perspect Biol. 4**,** a008425.

Kaartinen, V., Cui, X. M., Heisterkamp, N., Groffen, J., Shuler, C. F., 1997. Transforming growth factor-beta3 regulates transdifferentiation of medial edge epithelium during palatal fusion and associated degradation of the basement membrane. Dev Dyn. 209**,** 255-60.

Kaartinen, V., Voncken, J. W., Shuler, C., Warburton, D., Bu, D., Heisterkamp, N., Groffen, J., 1995. Abnormal lung development and cleft palate in mice lacking TGF-beta 3 indicates defects of epithelial-mesenchymal interaction. Nat Genet. 11**,** 415-21.

Kalter, H., Warkany, J., 1961. Experimental production of congenital malformations in strains of inbred mice by maternal treatment with hypervitaminosis A. The American journal of pathology. 38**,** 1-21.

Kaplan, E. N., 1975. The occult submucous cleft palate. The Cleft palate journal. 12**,** 356-68.

Katori, Y., Rodriguez-Vazquez, J. F., Kawase, T., Murakami, G., Cho, B. H., Abe, S., 2011. Early fetal development of hard tissue pulleys for the human superior oblique and tensor veli palatini muscles. Ann Anat. 193**,** 127-33.

Kitamura, H., 1966. Epithelial remnants and pearls in the secondary palate in the human abortus: a contribution to the study of the mechanism of cleft palate formation. The Cleft palate journal. 3**,** 240-57.

Kondo, S., Schutte, B. C., Richardson, R. J., Bjork, B. C., Knight, A. S., Watanabe, Y., Howard, E., de Lima, R. L., Daack-Hirsch, S., Sander, A., McDonald-McGinn, D. M., Zackai, E. H., Lammer, E. J., Aylsworth, A. S., Ardinger, H. H., Lidral, A. C., Pober, B. R., Moreno, L., Arcos-Burgos, M., Valencia, C., Houdayer, C., Bahuau, M., Moretti-Ferreira, D., Richieri-Costa, A., Dixon, M. J., Murray, J. C., 2002. Mutations in IRF6 cause Van der Woude and popliteal pterygium syndromes. Nat Genet. 32**,** 285-9.

Kraus, B. S., Kitamura, H., Latham, R. A., 1966. Atlas of developmental anatomy of the face, with special reference to normal and cleft lip and palate. Hoeber Medical Division, New York,.

Lee, S. H., Bedard, O., Buchtova, M., Fu, K., Richman, J. M., 2004. A new origin for the maxillary jaw. Dev Biol. 276**,** 207-24.

Loeys, B. L., Chen, J., Neptune, E. R., Judge, D. P., Podowski, M., Holm, T., Meyers, J., Leitch, C. C., Katsanis, N., Sharifi, N., Xu, F. L., Myers, L. A., Spevak, P. J., Cameron, D. E., De Backer, J., Hellemans, J., Chen, Y., Davis, E. C., Webb, C. L., Kress, W., Coucke, P., Rifkin, D. B., De Paepe, A. M., Dietz, H. C., 2005. A syndrome of altered cardiovascular, craniofacial, neurocognitive and skeletal development caused by mutations in TGFBR1 or TGFBR2. Nat Genet. 37**,** 275-81.

Loeys, B. L., Dietz, H. C., 1993. Loeys-Dietz Syndrome.

MacDonald, M. E., Abbott, U. K., Richman, J. M., 2004. Upper beak truncation in chicken embryos with the cleft primary palate mutation is due to an epithelial defect in the frontonasal mass. Dev Dyn. 230**,** 335-49.

Mangold, E., Ludwig, K. U., Birnbaum, S., Baluardo, C., Ferrian, M., Herms, S., Reutter, H., de Assis, N. A., Chawa, T. A., Mattheisen, M., Steffens, M., Barth, S., Kluck, N., Paul, A., Becker, J., Lauster, C., Schmidt, G., Braumann, B., Scheer, M., Reich, R. H., Hemprich, A., Potzsch, S., Blaumeiser, B., Moebus, S., Krawczak, M., Schreiber, S., Meitinger, T., Wichmann, H. E., Steegers-Theunissen, R. P., Kramer, F. J., Cichon, S., Propping, P., Wienker, T. F., Knapp, M., Rubini, M., Mossey, P. A., Hoffmann, P., Nothen, M. M., 2010. Genome-wide association study identifies two susceptibility loci for nonsyndromic cleft lip with or without cleft palate. Nat Genet. 42**,** 24-6.

Marazita, M. L., 2012. The evolution of human genetic studies of cleft lip and cleft palate. Annu Rev Genomics Hum Genet. 13**,** 263-83.

Marcano, A. C., Doudney, K., Braybrook, C., Squires, R., Patton, M. A., Lees, M. M., Richieri-Costa, A., Lidral, A. C., Murray, J. C., Moore, G. E., Stanier, P., 2004. TBX22 mutations are a frequent cause of cleft palate. J Med Genet. 41**,** 68-74.

Mato, M., Aikawa, E., Smiley, G. R., 1972. Invagination of human palatal epithelium prior to contact. The Cleft palate journal. 9**,** 325-40.

Miettinen, P. J., Chin, J. R., Shum, L., Slavkin, H. C., Shuler, C. F., Derynck, R., Werb, Z., 1999. Epidermal growth factor receptor function is necessary for normal craniofacial development and palate closure. Nat Genet. 22**,** 69-73.

Mittal, M., Maheshwari, N., Ahlawat, K., Sharma, V., Sultan, A., Chopra, R., 2012. Detection of orbicularis oris muscle defects in first degree relatives of cleft lip children using ultrasound. Journal of the Indian Society of Pedodontics and Preventive Dentistry. 30**,** 237-41.

Mogass, M., Bringas, P., Jr., Shuler, C. F., 2000. Characterization of desmosomal component expression during palatogenesis. The International journal of developmental biology. 44**,** 317-22.

Monteagudo, B., Labandeira, J., Cabanillas, M., Acevedo, A., Leon-Muinos, E., Toribio, J., 2012. Prevalence of milia and palatal and gingival cysts in Spanish newborns. Pediatric dermatology. 29**,** 301-5.

Monteleone, L., McLellan, M. S., 1964. Epstein's Pearls (Bohn's Nodules) of the Palate. Journal of oral surgery, anesthesia, and hospital dental service. 22**,** 301-4.

Mossey, P. A., Castilla, E. E., Global registry and database on craniofacial anomalies. World Health Organization, Geneva, 2003.

Mossey, P. A., Little, J., Epidemiology of oral clefts: an international perspective. In: D. F. Wyszynski, (Ed.), Cleft lip and palate: from origins to treatment. Oxford University Press, New York, 2002, pp. 127-158.

Mossey, P. A., Little, J., Munger, R. G., Dixon, M. J., Shaw, W. C., 2009. Cleft lip and palate. Lancet. 374**,** 1773-85.

Murray, J. C., Schutte, B. C., 2004. Cleft palate: players, pathways, and pursuits. J Clin Invest. 113**,** 1676-8.

Nawshad, A., 2008. Palatal seam disintegration: to die or not to die? that is no longer the question. Dev Dyn. 237**,** 2643-56.

O'Rahilly, R., Muller, F., 2007. The development of the neural crest in the human. J Anat. 211**,** 335-51.

O'Rahilly, R., Muller, F., 2010. Developmental stages in human embryos: revised and new measurements. Cells, tissues, organs. 192**,** 73-84.

Ooë, T., 1981. Human Tooth and Dental Arch Development. Ishiyaku Publishers Inc., Tokyo.

Oostrom, C. A., Vermeij-Keers, C., Gilbert, P. M., van der Meulen, J. C., 1996. Median cleft of the lower lip and mandible: case reports, a new embryologic hypothesis, and subdivision. Plast Reconstr Surg. 97**,** 313-20.

Park, J. W., McIntosh, I., Hetmanski, J. B., Jabs, E. W., Vander Kolk, C. A., Wu-Chou, Y. H., Chen, P. K., Chong, S. S., Yeow, V., Jee, S. H., Park, B. Y., Fallin, M. D., Ingersoll, R., Scott, A. F., Beaty, T. H., 2007. Association between IRF6 and nonsyndromic cleft lip with or without cleft palate in four populations. Genet Med. 9**,** 219-27.

Passos-Bueno, M. R., Ornelas, C. C., Fanganiello, R. D., 2009. Syndromes of the first and second pharyngeal arches: A review. Am J Med Genet A. 149A**,** 1853-9.

Paula, J. D., Dezan, C. C., Frossard, W. T., Walter, L. R., Pinto, L. M., 2006. Oral and facial inclusion cysts in newborns. The Journal of clinical pediatric dentistry. 31**,** 127-9.

Pauws, E., Hoshino, A., Bentley, L., Prajapati, S., Keller, C., Hammond, P., Martinez-Barbera, J. P., Moore, G. E., Stanier, P., 2009a. Tbx22null mice have a submucous cleft palate due to reduced palatal bone formation and also display ankyloglossia and choanal atresia phenotypes. Hum Mol Genet. 18**,** 4171-9.

Pauws, E., Moore, G. E., Stanier, P., 2009b. A functional haplotype variant in the TBX22 promoter is associated with cleft palate and ankyloglossia. J Med Genet. 46**,** 555-61.

Poswillo, D., 1974. The pattogenesis of submucous cleft palate. Scandinavian journal of plastic and reconstructive surgery. 8**,** 34-41.

Proetzel, G., Pawlowski, S. A., Wiles, M. V., Yin, M., Boivin, G. P., Howles, P. N., Ding, J., Ferguson, M. W., Doetschman, T., 1995. Transforming growth factor-beta 3 is required for secondary palate fusion. Nat Genet. 11**,** 409-14.

Rood, S. R., 1973. The morphology of M. tensor veli palatini in the five-month human fetus. Am J Anat. 138**,** 191-5.

Sadler, T. W., Langman, J., 2010a. Langman's medical embryology. Wolters Kluwer Lippincott Williams & Wilkins, Philadelphia.

Sadler, T. W., Langman, J. M. e., 2010b. Langman's medical embryology. Wouters Kluwer/Lippincott Williams & Wilkins, Philadelphia.

Sagai, T., Amano, T., Tamura, M., Mizushina, Y., Sumiyama, K., Shiroishi, T., 2009. A cluster of three long-range enhancers directs regional Shh expression in the epithelial linings. Development. 136**,** 1665-74.

Saunders, I. D., 1972. Bohn's nodules. A case report. British dental journal. 132**,** 457-8.

Scambler, P. J., 2000. The 22q11 deletion syndromes. Hum Mol Genet. 9**,** 2421-6.

Scapoli, L., Palmieri, A., Martinelli, M., Pezzetti, F., Carinci, P., Tognon, M., Carinci, F., 2005. Strong evidence of linkage disequilibrium between polymorphisms at the IRF6 locus and nonsyndromic cleft lip with or without cleft palate, in an Italian population. Am J Hum Genet. 76**,** 180-3.

Seif, S., Dellon, A. L., 1978. Anatomic relationshiphs between the human levator and tensor veli palatini and the eustachian tube. Cleft Palate J. 15**,** 329-36.

Sevel, D., 1981. A reappraisal of the origin of human extraocular muscles. Ophthalmology. 88**,** 1330-8.

Shah, R. M., Chaudhry, A. P., 1974. Ultrastructural observations on closure of the soft palate in hamsters. Teratology. 10**,** 17-29.

Shuler, C. F., 1995. Programmed cell death and cell transformation in craniofacial development. Critical reviews in oral biology and medicine : an official publication of the American Association of Oral Biologists. 6**,** 202-17.

Singh, I., 2005. Atlas of human anatomy : with CD supplement. Jaypee Brothers ; Tunbridge Wells : Anshan, New Delhi.

Singh, K. K., Rommel, K., Mishra, A., Karck, M., Haverich, A., Schmidtke, J., Arslan-Kirchner, M., 2006. TGFBR1 and TGFBR2 mutations in patients with features of Marfan syndrome and Loeys-Dietz syndrome. Hum Mutat. 27**,** 770-7.

Smiley, G. R., 1972. A possible genesis for cleft palate formation. Plastic and reconstructive surgery. 50**,** 390-4.

Smiley, G. R., 1975. A histological study of the formation and development of the soft palate in mice and man. Archives of oral biology. 20**,** 297-8.

Smiley, G. R., Koch, W. E., 1975. A comparison of secondary palate development with different in vitro techniques. Anat Rec. 181**,** 711-23.

Sperber, G. H., Guttman, G. D., 2010. Craniofacial embryogenetics and development. People's Medical Pub. House USA, 2010, Shelton, CT.

Streeter, G. H., 1920. Weight, sitting height, head size, foot length, and menstrual age of the human embryo. Contrib Embryol. 11**,** 143.

Suga, K., Muramatsu, K., Uchiyama, T., Takano, N., Shibahara, T., 2010. Congenital epidermoid cyst arising in soft palate near uvula: a case report. The Bulletin of Tokyo Dental College. 51**,** 207-11.

Sun, D., Baur, S., Hay, E. D., 2000. Epithelial-mesenchymal transformation is the mechanism for fusion of the craniofacial primordia involved in morphogenesis of the chicken lip. Dev Biol. 228**,** 337-49.

Suphapeetiporn, K., Tongkobpetch, S., Siriwan, P., Shotelersuk, V., 2007. TBX22 mutations are a frequent cause of non-syndromic cleft palate in the Thai population. Clin Genet. 72**,** 478-83.

Walker, B. E., Crain, B., Jr., 1960. Effects of hypervitaminosis A on palate development in two strains of mice. The American journal of anatomy. 107**,** 49-58.

Weatherley-White, R. C., Sakura, C. Y., Jr., Brenner, L. D., Stewart, J. M., Ott, J. E., 1972. Submucous cleft palate. Its incidence, natural history, and indications for treatment. Plastic and reconstructive surgery. 49**,** 297-304.

Wood, P. J., Kraus, B. S., 1962. Prenatal development of the human palate. Some histological observations. Arch Oral Biol. 7**,** 137-50.

Xu, X., Han, J., Ito, Y., Bringas, P., Jr., Urata, M. M., Chai, Y., 2006. Cell autonomous requirement for Tgfbr2 in the disappearance of medial edge epithelium during palatal fusion. Dev Biol. 297**,** 238-48.

Zucchero, T. M., Cooper, M. E., Maher, B. S., Daack-Hirsch, S., Nepomuceno, B., Ribeiro, L., Caprau, D., Christensen, K., Suzuki, Y., Machida, J., Natsume, N., Yoshiura, K., Vieira, A. R., Orioli, I. M., Castilla, E. E., Moreno, L., Arcos-Burgos, M., Lidral, A. C., Field, L. L., Liu, Y. E., Ray, A., Goldstein, T. H., Schultz, R. E., Shi, M., Johnson, M. K., Kondo, S., Schutte, B. C., Marazita, M. L., Murray, J. C., 2004. Interferon regulatory factor 6 (IRF6) gene variants and the risk of isolated cleft lip or palate. N Engl J Med. 351**,** 769-80.